

Worst-case low-rank approximations

Anya Fries

*Seminar for Statistics
ETH Zürich
Zürich, Switzerland*

ANYA.FRIES@STAT.MATH.ETHZ.CH

Markus Reichstein

*Max Planck Institute for Biogeochemistry
Jena, Germany*

MREICHSTEIN@BGC-JENA.MPG.DE

David Blei

*Department of Computer Science and Department of Statistics
Columbia University
New York, USA*

DAVID.BLEI@COLUMBIA.EDU

Jonas Peters

*Seminar for Statistics
ETH Zürich
Zürich, Switzerland*

JONAS.PETERS@STAT.MATH.ETHZ.CH

Abstract

Real-world data in health, economics, and environmental sciences are often collected across heterogeneous domains (such as hospitals, regions, or time periods). In such settings, distributional shifts can make standard PCA unreliable, in that, for example, the leading principal components may explain substantially less variance in unseen domains than in the training domains. Existing approaches (such as FairPCA) have proposed to consider worst-case (rather than average) performance across multiple domains. This work develops a unified framework, called wcPCA, applies it to other objectives (resulting in the novel estimators such as `norm-minPCA` and `norm-maxRegret`, which are better suited for applications with heterogeneous total variance) and analyzes their relationship. We prove that for all objectives, the estimators are worst-case optimal not only over the observed source domains but also over all target domains whose covariance lies in the convex hull of the (possibly normalized) source covariances. We establish consistency and asymptotic worst-case guarantees of empirical estimators. We extend our methodology to matrix completion, another problem that makes use of low-rank approximations, and prove approximate worst-case optimality for inductive matrix completion. Simulations and two real-world applications on ecosystem-atmosphere fluxes demonstrate marked improvements in worst-case performance, with only minor losses in average performance.

Keywords: distribution generalization, worst-case optimality, principal component analysis, matrix completion, low-rank approximation

1 Introduction

Real-world data frequently originate from multiple heterogeneous domains, characterized by distinct statistical properties or underlying structures. For example, medical data collected from different hospitals or environmental data spanning different ecosystems and time periods often exhibit distributional shifts. Traditional dimensionality reduction methods, such

as principal components analysis (PCA), generally implicitly assume homogeneity across domains. When this assumption is violated, pooled representations can fail to generalize, for example, explaining substantially less variance in unseen domains.

PCA summarizes data in a lower-dimensional subspace chosen to maximize explained variance (or, equivalently, to minimize ℓ_2 -reconstruction error). Given a random (row) vector $\mathbf{x} \in \mathbb{R}^{1 \times p}$ with zero mean and covariance matrix $\Sigma := \mathbb{E}[\mathbf{x}^\top \mathbf{x}] \in \mathbb{R}^{p \times p}$, we say that an orthonormal matrix $V_k^* \in \mathbb{R}^{p \times k}$ solves *rank- k population PCA* if

$$V_k^* \in \arg \max_{V \in \mathcal{O}_{p \times k}} \text{Tr}(V^\top \Sigma V), \tag{1}$$

where $\mathcal{O}_{p \times k}$ denotes the space of all $p \times k$ -dimensional orthonormal matrices (in practice, one considers sample covariance matrices instead). In the multi-domain setting, where we observe data in different domains e (corresponding to different covariance matrices Σ_e) no single covariance characterizes the data and the question arises how to take the different domains into consideration. Intuitively, pooling all samples to form a single sample covariance matrix ignores domain-specific variability, while treating each domain independently discards common structure. This work investigates the implications of replacing $\text{Tr}(V^\top \Sigma V)$ in (1) by a term aggregating over the source domains; for example, $\text{Tr}(V^\top \sum_e w_e \Sigma_e V)$ (corresponding to a pooling approach) or $\min_e \text{Tr}(V^\top \Sigma_e V)$ (corresponding to a worst-case approach). These objectives generally yield different answers (see, for example, Figures 1 and 2).

Moreover, this work shows that the different objectives yield different performances on test domains, too: for example, some, but not all, satisfy robustness guarantees that extend beyond the observed source domains (see Section 3.1 for details). To illustrate this point empirically, we consider daily averages of FLUXNET data (Pastorello et al., 2020), a global network of eddy covariance towers that measure biosphere–atmosphere exchanges of CO₂ (e.g., net ecosystem exchange, gross primary production), water vapor, and energy. We treat the TransCom 3 regions (a standard partition of the globe into large-scale climate zones (Gurney et al., 2002, 2004)) as domains, and select five of them as source domains. We solve PCA on the pooled source data (`poolPCA`) and compare it with one of the methods proposed in this paper (`norm-maxRegret`), a worst-case low-rank approximation. We consider two PCs (see Figure C.i for a justification). The proportion of explained variance is then evaluated for each source and target regions. Figure 1 shows that `norm-maxRegret` improves upon `poolPCA` in worst-case error (with only a moderate reduction in terms of average performance). Section 6.1 further shows that similar results hold for other splits into source and target domains, too; it also provides further details on the experimental setup.

We extend the worst-case framework to matrix completion, motivated by the following connection to PCA. For a fixed $k < p$, PCA is an instance of low-rank approximation: in the finite-sample setting, it solves $\min_{V \in \mathcal{O}_{p \times k}} \|X - XVV^\top\|_F^2$, where $X \in \mathbb{R}^{n \times p}$ is a data matrix (so that XV and V^\top act as left and right factors, respectively). Low-rank approximations are also used to tackle the problem of matrix completion (Candès and Plan, 2010; Candès and Recht, 2012): here, a partially observed matrix is approximated by a low-rank factorization in order to predict the missing entries (e.g., Jain et al., 2013). However, traditional matrix completion approaches—much like PCA—implicitly assume

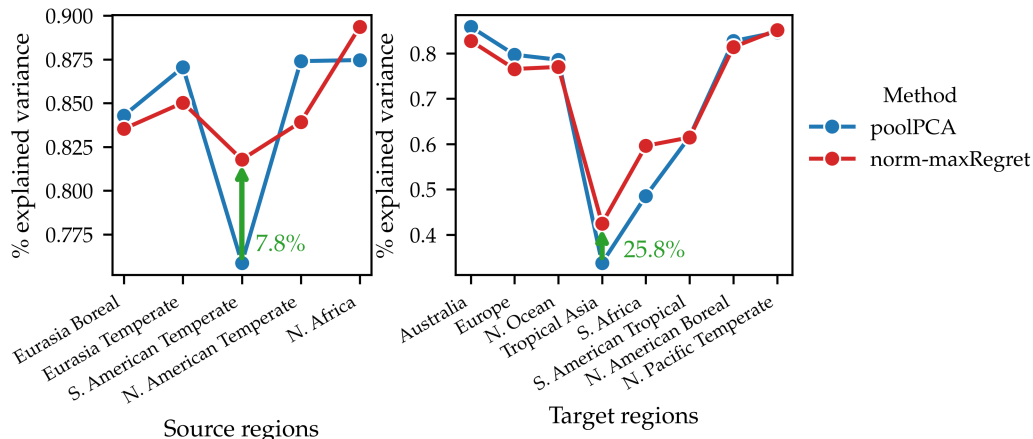


Figure 1: *Proportion of explained variance by poolPCA and norm-maxRegret in the FLUXNET example on source (left) and target (right) regions (for one specific split). Unlike poolPCA, which optimizes a pooled explained variance, norm-maxRegret optimizes a worst-case criterion over the source domains, which, here, yields a worst-case improvement of 7.8%. Section 3.1 proves that this choice comes with a worst-case improvement over a larger class of target domains, too. Indeed, in this example, the worst-case explained variance over the target domains improves by 25.8%. (Over 20 different splits, the median relative increase in worst-case improvements equal 25.6% and 16.6% for source and target domains, respectively; the median decrease in average performance for source domains equals 7.5%; see Section 6.1 for more details.)*

that the latent structure is homogeneous across all samples. We thus apply the worst-case principle to matrix completion and propose to learn a shared representation that minimizes worst-case reconstruction error (on the observed entries) across the source domains, and then use the shared factor for inductive matrix completion in a new, partially observed target domain. Section 4 proves that, when the source domains are fully observed, we obtain analogous robustness guarantees to those of the worst-case PCA formulations, up to an approximation factor.

1.1 Related work

Domain generalization in prediction. Domain generalization in prediction has been studied extensively. One approach considers adversarial robustness, where performance is optimized under worst-case training scenarios. Examples include maximin effects in regression (Meinshausen and Bühlmann, 2015; Guo, 2024), Magging (Bühlmann and Meinshausen, 2016), Distributionally Robust Optimization (DRO) (Ben-Tal et al., 2013; Duchi and Namkoong, 2019; Sinha et al., 2017), Group DRO (Sagawa et al., 2020; Hu et al., 2018), and maximum risk minimization (maxRM) (Freni et al., 2025). These approaches focus on predictive risk, whereas our work studies worst-case robustness for unsupervised dimensionality reduction.

Fair PCA. Several extensions of PCA have been proposed to address heterogeneous domains, especially in the context of fairness. Fair principal component analysis (Fair PCA), first proposed by Samadi et al. (2018), aims to reduce disparities in reconstruction error across groups, which can also be interpreted as domains. Samadi et al. (2018) consider two domains, and minimize the maximum increase in reconstruction error incurred by using a shared projection instead of the domain-specific optimal projection. For multiple domains, this objective is often referred to as the disparity error or regret (see Section 2.2.3). Kamani et al. (2022) study trade-offs between reconstruction accuracy and fairness constraints, while Zalcberg and Wiesel (2021) introduce fair robust PCA and fair sparse PCA. Within a broader multi-criteria dimensionality reduction framework, Tantipongpipat et al. (2019) define Fair PCA as maximizing worst-case explained variance (discussed in Section 2.2.1). These objectives have motivated algorithmic developments, including those of Babu and Stoica (2023). However, all of these approaches target fairness (i.e., in-sample guarantees), whereas our framework addresses out-of-sample guarantees.

Stable and common PCA. Beyond fairness, Wang et al. (2025) seek robustness guarantees across domains and study a Group DRO formulation of PCA with the Fantope relaxation, termed StablePCA. While they focus on the optimization algorithm, we focus on explicit out-of-sample guarantees (including stronger results for the population case and both consistency and robustness guarantees for the estimators). We also consider a broader class of worst-case objectives, analyze their relationship, and extend the framework to matrix completion. Other multi-domain PCA frameworks, such as the one proposed by Puchhammer et al. (2024), accommodate heterogeneous data but yield domain-specific projections rather than a unified robust representation. Similarly, common PCA (Flury, 1986, 1987) and common empirical orthogonal functions (Hannachi et al., 2023) allow for heterogeneous data, but neither provide worst-case nor out-of-sample guarantees.

Matrix completion Matrix completion is well studied in the single-domain setting, where recovery guarantees are available under an incoherence assumption and assumptions on the sampling process of the observed entries (e.g., Candès and Plan, 2010; Candès and Recht, 2012; Jain et al., 2013). Inductive matrix enables completion for previously unseen rows or columns, for example by incorporating side information (Jain and Dhillon, 2013) or by estimating latent factors from partially observed entries in a learned low-rank model (Koren et al., 2009). Multi-domain extensions include fairness-aware non-negative matrix factorization (Kassab et al., 2024) and fairness-aware federated matrix factorization (Liu et al., 2022). These works, however, focus on group fairness rather than robustness across heterogeneous domains. To our knowledge, the results we present in Section 4.2 are the first explicit worst-case guarantees for (inductive) matrix completion.

1.2 Contributions and outline

We develop a unified framework for worst-case PCA and matrix completion. While related objectives have appeared in Fair PCA and in relaxed formulations such as StablePCA, these works either do not address out-of-sample robustness or focus on the optimization problem. Our framework clarifies the relationships between worst-case variance-based, reconstruction-based, and regret-based objectives, which—unlike in classical PCA—generally yield distinct

solutions. We prove that the resulting worst-case solutions generalize beyond the observed domains, more specifically, that they are worst-case optimal over all distributions whose covariances lie in the convex hull of the source covariances. The guarantees extend ideas from distributionally robust optimisation while requiring only second-moment information. We further provide finite-sample theory, proving consistency and asymptotic worst-case optimality of the empirical estimators. Simulations and a FLUXNET case study demonstrate improvements in worst-case performance with only minor losses on average.

The remainder of this work is organized as follows. Section 2.1 motivates worst-case PCA (wcPCA). Section 2.2 introduces and discusses the variants of the objective and links them to reconstruction error. Section 3.1 establishes the main robustness guarantees, which we extend to the finite-sample setting in Section 3.2. Section 4 broadens the framework to matrix completion with missing data. Section 5 illustrates the theory through simulations and Section 6 presents two real-world applications on ecosystem–atmosphere flux data. All proofs can be found in Appendix D.

1.3 Notation

Throughout the article, we make use of the following notation. For all $n \in \mathbb{N}_+$, we write $[n] := \{1, \dots, n\}$. Generally, non-bold lowercase letters (e.g., x) are used for deterministic row vectors, bold lowercase letters (e.g., \mathbf{x}) are used for random row vectors, and uppercase letters (e.g., X) are used for random matrices. For all matrices $X \in \mathbb{R}^{n \times p}$ (random or deterministic), the Frobenius norm of X is denoted by $\|X\|_F = \sqrt{\sum_{i=1}^n \sum_{j=1}^p X_{ij}^2} = \sqrt{\text{Tr}(X^\top X)} = \sqrt{\sum_{i=1}^{\min\{n,p\}} \sigma_i^2(X)}$, where $\sigma_i(X)$ denotes singular values of X and $\text{Tr}(\cdot)$ the trace. For all $x \in \mathbb{R}^p$, $\text{diag}(x) \in \mathbb{R}^{p \times p}$ is the matrix formed with x on the diagonal and 0s elsewhere. The set of $p \times k$ matrices with orthonormal columns is denoted $\mathcal{O}_{p \times k} := \{V \in \mathbb{R}^{p \times k} \mid V^\top V = I_k\}$. The convex hull of a set S contained in a real vector space, denoted by $\text{conv}(S)$, is the set of all convex combinations of points in S , that is, $\text{conv}(S) := \{\sum_{i=1}^k \alpha_i x_i \mid x_i \in S, \alpha_i \geq 0, \sum_{i=1}^k \alpha_i = 1, k \in \mathbb{N}\}$.

2 Worst-case PCA and its variants

2.1 Setting and motivation

Given data from source domains, the goal is to learn low-dimensional representations that explain variance across these domains and on new (possibly unseen) target domains. We first consider a population setting, i.e., in each source domain, we are given the whole distribution; we discuss the finite-sample case in Section 3.2.

Setting 1 (Source domains) *Let $\mathcal{E} := \{1, \dots, E\}$ denote a set of E source domains. For all $e \in \mathcal{E}$, let $\mathbf{x}_e \in \mathbb{R}^{1 \times p}$ be a random row vector drawn from a distribution P_e such that $\mathbb{E}_{P_e}[\mathbf{x}_e] = 0$ and the covariance $\Sigma_e := \mathbb{E}_{P_e}[\mathbf{x}_e^\top \mathbf{x}_e] \in \mathbb{R}^{p \times p}$ exists and has strictly positive trace. For each $e \in \mathcal{E}$, let $w_e > 0$ denote the probability¹ that an observation comes from domain e , where the domain assignment is independent of all other randomness and $\sum_{e \in \mathcal{E}} w_e = 1$. The domain label associated with each observation is assumed to be observed.*

1. All methods and theoretical results developed in this paper apply both when domains are sampled randomly according to $(w_e)_{e \in \mathcal{E}}$ and when the domain sequence is deterministic.

A standard approach, which we refer to as `poolPCA`, is to pool all domains. This is often done implicitly, for example, when the domain structure is ignored. More concretely, we say $V_k^{\text{pool}} \in \mathcal{O}_{p \times k}$ solves *rank- k poolPCA* if it maximizes the average variance, i.e., it solves PCA for $\Sigma_{\text{pool}} := \sum_{e \in \mathcal{E}} w_e \Sigma_e$. Throughout the paper, we omit the subscript k whenever the rank is clear from context. One can also solve PCA in each domain. For each $e \in \mathcal{E}$, let $V_k^{*,e} \in \mathcal{O}_{p \times k}$ denote a rank- k PCA solution. There is no canonical way to combine these into a single representation, but one can consider a conservative option and select the solution from the domain that achieves the minimal explained variance. We say V_k^{sep} solves *rank- k sepPCA* (separate PCA) if

$$V_k^{\text{sep}} := V_k^{*,e_0} \quad \text{with} \quad e_0 := \arg \min_{e \in \mathcal{E}} \text{Tr} \left((V_k^{*,e})^\top \Sigma_e V_k^{*,e} \right),$$

where we choose e_0 to be the smallest index minimizing the objective.

Neither of these two baselines is necessarily optimal for maximizing explained variance across domains. When evaluated on the observed source domains, the pooled and separate solutions can perform poorly in the worst case and Section 5.1 demonstrates that the same may hold when these solutions are applied in test domains. The following example illustrates this point and motivates `wcPCA`, which explicitly optimizes for worst-case performance across domains.

Example 1 Consider two domains $\mathcal{E} := \{1, 2\}$, where observations are drawn from each domain with equal probability, that is, $w_1 = w_2$. The distribution in each domain is a zero-mean Gaussian with population covariances

$$\Sigma_1 := \text{diag}(0.9, 0.1, 0) \quad \text{and} \quad \Sigma_2 := \text{diag}(0, 0.4, 0.6),$$

respectively; the example is illustrated in Figure 2.

Rank-1 `poolPCA` considers $\Sigma_{\text{pool}} = \frac{1}{2}(\Sigma_1 + \Sigma_2)$ and yields $V^{\text{pool}} = (1, 0, 0)^\top$, while solving PCA separately in each (source) domain gives $(1, 0, 0)^\top$ for domain 1 and $(0, 0, 1)^\top$ for domain 2; selecting the solution from the domain with minimal explained variance yields $V^{\text{sep}} = (0, 0, 1)^\top$. V^{pool} and V^{sep} , respectively, explain 45% and 30% of the average covariance Σ_{pool} . However, both perform poorly (0% explained variance) in the respective worst-case source domain. This occurs because V^{pool} and V^{sep} are both orthogonal to the support of one of the domains, thus capturing no variance in that domain.

In contrast, the `wcPCA` variants explicitly optimize worst-case performance across domains. In particular, `minPCA` (Definition 1, below) is solved by $V^{\text{minPCA}} = \frac{1}{\sqrt{5}}(\sqrt{2}, 0, \sqrt{3})^\top$, which explains 36% of variance in both domains and `maxRegret` (Definition 3, below) is solved by $V^{\text{minPCA}} = \frac{1}{\sqrt{5}}(\sqrt{3}, 0, \sqrt{2})^\top$, which explains at least 24% of variance. Thus, while the explained variance with respect to the pooled covariance Σ_{pool} is comparable to that of V^{sep} and V^{pool} , they achieve strictly positive percentage of explained variance in the worst-case source domain.

We will see in Section 3.1 that this improvement is not restricted to the source domains: we prove that several variants of `wcPCA` (including `minPCA` and `maxRegret`) are worst-case optimal over all domains whose covariances lie in the convex hull of the source covariances.

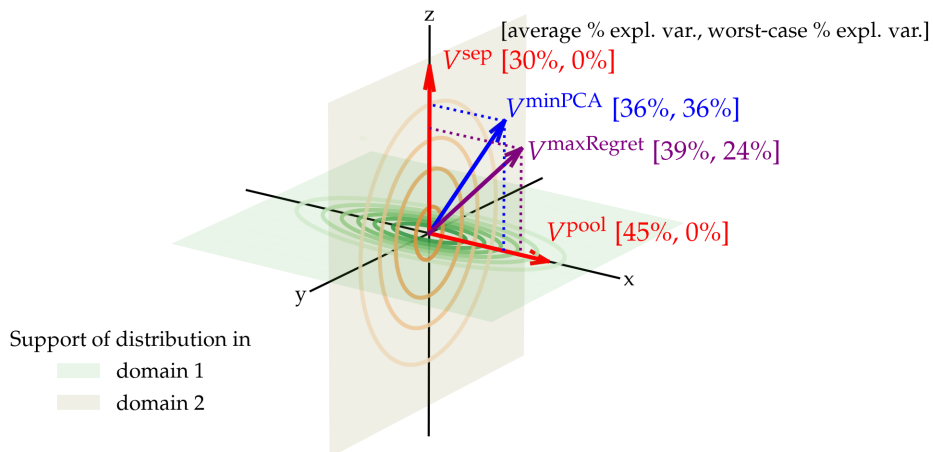


Figure 2: *Visualization of possible solutions to the rank-1 approximation problem in a specific example.* The figure shows contour plots of two distributions $\mathcal{N}(0, \Sigma_1)$ (green) and $\mathcal{N}(0, \Sigma_2)$ (orange), together with their supports (shaded planes). The methods `poolPCA`, `sepPCA`, `minPCA`, and `maxRegret` describe different ways to aggregate over different source domains in the objective function (see Section 2.2 for details); their solutions are denoted by V^{pool} , V^{sep} , V^{minPCA} , and $V^{\text{maxRegret}}$, respectively (the values in parentheses indicate the pooled and worst-case explained variance). For example, V^{pool} and V^{sep} explain 0% of variance in the worst-case domain, as they are orthogonal to the support of that domain. In contrast, V^{minPCA} maximizes the worst case explained variance (resulting in 36%) and $V^{\text{maxRegret}}$ explains at least 24% of variance in each domain. Details are provided in Example 1.

2.2 Variants of wcPCA

We now formally introduce some variants of wcPCA. More concretely, the objective may focus on maximizing variance or minimizing reconstruction error and the source covariances may or may not be normalized prior to optimization. This leads to four variants: `minPCA`, `norm-minPCA`, `maxRCS`, and `norm-maxRCS`. In addition, we introduce the regret-based formulations `maxRegret` and `norm-maxRegret`, which evaluate performance relative to each domain’s own optimal subspace. The objectives `minPCA` and `maxRegret` have been proposed previously; only `minPCA` has been considered as a “distributionally robust” PCA by Wang et al. (2025) – but no explicit theoretical guarantees have been provided. Table 1 provides an overview of these variants.

For classical PCA, the solution spaces of many of these variants coincide² but we see in Section 2.2.5 that this is generally not the case in the multi-domain setting (Section 2.2.6 discusses intuition about when to use which objective). Section 3.1 proves that all of these variants satisfy worst-case optimality guarantees.

2. E.g., for a covariance matrix Σ , the sets of solutions to rank- k PCA on Σ and $\Sigma/\text{Tr}(\Sigma)$ are the same, as $\arg \max_{V \in \mathcal{O}_{p \times k}} \{\text{Tr}(V^T \Sigma V)\} = \arg \max_{V \in \mathcal{O}_{p \times k}} \{\text{Tr}(V^T \Sigma V)/\text{Tr}(\Sigma)\}$.

| Normalized | Objective function | | | | | |
|------------|--------------------|----------------------|-------------|----------|----------------|--------|
| | Explained variance | Reconstruction error | | Regret | | |
| | (Def. 1) | (Def. 2) | | (Def. 3) | | |
| No | minPCA | \neq | maxRCS | \neq | maxRegret | \neq |
| | \neq | | \neq | | \neq | |
| Yes | norm-minPCA | $=$ | norm-maxRCS | \neq | norm-maxRegret | \neq |

Table 1: The six worst-case PCA formulations considered in this work: three objectives (explained variance, reconstruction error, and regret) combined with two normalization choices (normalized vs. unnormalized). The symbols $=$ and \neq indicate whether the solutions coincide (see Theorem 5). The equality holds if the methods are applied to the full (and usually unknown) distribution or to its empirical counterpart.

2.2.1 EXPLAINED VARIANCE

Let the explained variance and normalized (or proportion of) explained variance of a subspace V for a distribution P with covariance Σ be

$$\mathcal{L}_{\text{var}}(V; P) := \text{Tr}(V^\top \Sigma V), \quad \mathcal{L}_{\text{normVar}}(V; P) := \frac{\text{Tr}(V^\top \Sigma V)}{\text{Tr}(\Sigma)}. \quad (2)$$

Definition 1 (minPCA) Consider Setting 1. An orthonormal matrix $V^* \in \mathcal{O}_{p \times k}$ solves rank- k minPCA (resp. norm-minPCA) if

$$V^* \in \arg \max_{V \in \mathcal{O}_{p \times k}} \left\{ \min_{e \in \mathcal{E}} \mathcal{L}(V; P_e) \right\},$$

where $\mathcal{L} = \mathcal{L}_{\text{var}}$ (resp. $\mathcal{L} = \mathcal{L}_{\text{normVar}}$).

With respect to the standard metric induced by the Frobenius norm, $\mathcal{O}_{p \times k}$ is compact as a closed and bounded subset of $\mathbb{R}^{p \times k}$ (by Heine-Borel), and the objective function is continuous. Hence, the maximum is attained.

2.2.2 RECONSTRUCTION ERROR

PCA does not only maximize explained variance, it also minimizes the expected reconstruction error among all rank- k approximations. Specifically, for a random vector $\mathbf{x} \in \mathbb{R}^{1 \times p}$ drawn from distribution P with covariance matrix $\Sigma := \mathbb{E}_P[\mathbf{x}^\top \mathbf{x}]$, it holds that $\arg \max_{V \in \mathcal{O}_{p \times k}} \text{Tr}(V^\top \Sigma V) = \arg \min_{V \in \mathcal{O}_{p \times k}} \mathbb{E}_{\mathbf{x} \sim P} [\|\mathbf{x} - \mathbf{x} V V^\top\|_2^2]$. We now define a worst-case objective corresponding to the right-hand side of this equation. To do so, we use the following notation for the expected unnormalized and normalized reconstruction losses:

$$\mathcal{L}_{\text{RCS}}(V; P) := \mathbb{E}_{\mathbf{x} \sim P} [\|\mathbf{x} - \mathbf{x} V V^\top\|_2^2], \quad \mathcal{L}_{\text{normRCS}}(V; P) := \frac{\mathbb{E}_{\mathbf{x} \sim P} [\|\mathbf{x} - \mathbf{x} V V^\top\|_2^2]}{\mathbb{E}_{\mathbf{x} \sim P} [\|\mathbf{x}\|_2^2]}. \quad (3)$$

Definition 2 (maxRCS) Consider Setting 1. An orthonormal matrix $V^* \in \mathcal{O}_{p \times k}$ solves rank- k maxRCS (resp. norm-maxRCS) if

$$V^* \in \arg \min_{V \in \mathcal{O}_{p \times k}} \left\{ \max_{e \in \mathcal{E}} \mathcal{L}(V; P_e) \right\},$$

where $\mathcal{L} = \mathcal{L}_{\text{RCS}}$ (resp. $\mathcal{L} = \mathcal{L}_{\text{normRCS}}$).

2.2.3 REGRET

The two formulations introduced above optimize ‘absolute performance’ in the worst-case domain. Alternatively, we can assess performance with respect to each domain’s own optimal subspace. This leads to a regret-based formulation, which quantifies the increase in reconstruction error incurred by enforcing a common subspace across domains. Let the expected unnormalized and normalized regret be

$$\begin{aligned}\mathcal{L}_{\text{reg}}(V; P) &:= \mathcal{L}_{\text{RCS}}(V; P_e) - \min_{W \in \mathcal{O}_{p \times k}} \mathcal{L}_{\text{RCS}}(W; P_e), \\ \mathcal{L}_{\text{normReg}}(V; P) &:= \mathcal{L}_{\text{normRCS}}(V; P_e) - \min_{W \in \mathcal{O}_{p \times k}} \mathcal{L}_{\text{normRCS}}(W; P_e).\end{aligned}$$

We can now define a regret-based³ variant of wcPCA.

Definition 3 (maxRegret) *Consider Setting 1. An orthonormal matrix $V^* \in \mathcal{O}_{p \times k}$ solves rank- k maxRegret (resp. norm-maxRegret) if*

$$V^* \in \arg \min_{V \in \mathcal{O}_{p \times k}} \left\{ \max_{e \in \mathcal{E}} \mathcal{L}(V; P_e) \right\},$$

where $\mathcal{L} = \mathcal{L}_{\text{reg}}$ (resp. $\mathcal{L} = \mathcal{L}_{\text{normReg}}$).

2.2.4 ITERATIVE OPTIMIZATION

The PCA solution in (1) can be computed iteratively by sequentially selecting orthonormal directions that successively maximize explained variance in the remaining space. For PCA, this sequential procedure is equivalent to solving the joint optimization problem (1) and therefore yields an optimal solution (Jolliffe, 2002, Property A1, p.11). Sequential analogues can also be defined for minPCA and norm-minPCA by choosing orthonormal components iteratively to optimize worst-case explained variance. In contrast to classical PCA, however, this greedy construction generally fails to recover the optimal joint solution.

Proposition 4 (Sequential vs. joint optimization, informal) *In general, the subspace obtained by sequentially selecting directions to optimize the worst-case explained variance (resp. worst-case proportion of explained variance) does not coincide with the solution of the joint minPCA (resp. norm-minPCA) problem.*

A formal statement of the proposition and a counterexample are given in Appendix A.1.

When an ordered basis is required, we first compute the optimal subspace and then, starting from the full subspace, we iteratively remove the direction whose removal maximizes the worst-case explained variance of the remaining subspace. This construction yields an ordered basis consistent with the joint solution (Appendix A.2 provides further details).

3. Theorem 5 below proves that Definition 3 can equivalently be formulated using explained variance rather than reconstruction error.

2.2.5 RELATIONS BETWEEN THE wcPCA VARIANTS

For classical PCA the solution set does not depend on whether one optimizes for explained variance, reconstruction error, or their normalized versions. For the worst-case setting, Theorem 5 below proves that normalizing the objective can alter the solution set (statement (i)), equivalence between worst-case explained-variance and reconstruction-error formulations holds only for the normalized objectives (statement (ii)), and for regret-based objectives the solution set does not depend on whether regret is formulated using explained variance or reconstruction error (statement (iii)).

Theorem 5 (Relations between wcPCA variants) *Consider Setting 1. Then, the symbols $=$ and \neq in Table 1 represent whether the solutions coincide. More precisely, the following statements hold.*

- i) **Effect of normalization.** *Let $V^{\min PCA}$ and $V^{\text{norm-minPCA}}$ solve rank- k $\min PCA$ and norm-minPCA , respectively. In general, $V^{\min PCA}$ does not solve norm-minPCA and $V^{\text{norm-minPCA}}$ does not solve $\min PCA$. Analogous statements hold for $\max RCS$ versus norm-maxRCS and for $\max Regret$ versus norm-maxRegret .*
- ii) **Explained variance vs. reconstruction error.** *Let $V^{\min PCA}$ and $V^{\max RCS}$ solve rank- k $\min PCA$ and $\max RCS$, respectively. In general, $V^{\min PCA}$ does not solve $\max RCS$ and $V^{\max RCS}$ does not solve $\min PCA$. In contrast, the set of solutions to rank- k norm-minPCA coincides with the set of solutions to rank- k norm-maxRCS .*
- iii) **Regret.** *The set of solutions to the regret problem formulated using reconstruction error (as in Definition 3) coincides with that of the variance-based formulation, that is, with the solutions obtained by replacing \mathcal{L}_{RCS} with $-\mathcal{L}_{\text{var}}$ (or $\mathcal{L}_{\text{normRCS}}$ with $-\mathcal{L}_{\text{normVar}}$).*

2.2.6 PRACTICAL CONSIDERATIONS FOR CHOOSING THE OBJECTIVE

As summarized in Table 1, the various objectives lead to different sets of solutions. We now discuss some of the differences between the objectives and how factors such as scale heterogeneity and noise influence their behavior. We also discuss how worst-case objectives can be used diagnostically to assess domain heterogeneity.

Sensitivity to varying variances. The unnormalized objectives optimize worst-case explained variance or reconstruction error in the original units. As a consequence, domains with particularly small (resp. large) total variance $\text{Tr}(\Sigma_e)$ can dominate the objective of $\min PCA$ (resp. $\max RCS$). In particular, $\min PCA$ maximizes worst-case explained variance in absolute terms, so its solution may be entirely determined by a domain whose variance in every direction is smaller than that of any other domain. In contrast, the normalized variants norm-minPCA and norm-maxRCS optimize proportional explained variance or reconstruction error, which may result in a different worst-case domain and lead to a different solution. These normalized objectives are therefore less sensitive to differences in total variance and align with the interpretation of how much of each domain is explained, but unit comparability across domains is lost. Similarly, $\max Regret$ is not as sensitive to particularly large or small $\text{Tr}(\Sigma_e)$ either as it compares performance relative to domain-optimal subspaces.

Choosing between explained variance and reconstruction error. For the unnormalized objectives, `minPCA` and `maxRCS` can lead to different solutions. In contrast, the normalized objectives (`norm-minPCA` and `norm-maxRCS`), as well as the regret, produce identical solution sets under either formulation, eliminating the need for this decision and aligning more closely with standard PCA.

Effect of heterogeneous noise. When noise levels differ across domains, the regret provides a robust way to learn a common subspace even if the ultimate goal is to optimize explained variance or reconstruction error. Indeed, let us consider observations with different noise variances, that is, for all $e \in \mathcal{E}$ we observe

$$\mathbf{z}_e := \mathbf{x}_e + \sigma_e \boldsymbol{\varepsilon}_e, \quad \boldsymbol{\varepsilon}_e \sim N(0, I_p),$$

where \mathbf{x}_e is as in Setting 1 and for all $e, e' \in \mathcal{E}$, $\sigma_e > 0$ and $\boldsymbol{\varepsilon}_e$ is independent of $\boldsymbol{\varepsilon}_{e'}$ and \mathbf{x}_e . Then, \mathbf{z}_e has covariance $\Sigma_e + \sigma_e^2 I_p$. By slight abuse of notation, we say the problem is *noiseless* if $\sigma_e = 0, \forall e \in \mathcal{E}$; otherwise, we say that there is *heterogeneous noise*. Let us first consider the proposed methods applied to the population covariance matrices. For any $V \in \mathcal{O}_{p \times k}$ and $e \in \mathcal{E}$, the explained variance is $\text{Tr}(V^\top \Sigma_e V) + k\sigma_e^2$. Thus, domains with particularly high noise do not attain the minimum in `minPCA` but can influence the `maxRCS` solution. In contrast, the regret compares a common subspace V to the rank- k domain-optimal subspace $V_k^{e,*}$, so the noise terms cancel and the objective reduces to $\text{Tr}((V_k^{e,*})^\top \Sigma_e V_k^{e,*}) - \text{Tr}(V^\top \Sigma_e V)$. Consequently, heterogeneous noise affects the solutions of `minPCA` and `maxRCS` but not of `maxRegret`. Moreover, if each Σ_e is exactly rank- k , then $\text{Tr}((V_k^{e,*})^\top \Sigma_e V_k^{e,*}) = \text{Tr}(\Sigma_e)$ and minimizing the maximum regret is equivalent to minimizing the maximum reconstruction error in the noiseless setting (see proof of Theorem 5). For finitely many data, these statements may not hold precisely but in our simulations, the same qualitative patterns persist (see Section 5.1.4).

Worst-case losses as diagnostics tools. While Section 3.1 proves that the different `wcPCA` objectives come with out-of-distribution guarantees, the multi-domain losses can also be used diagnostically. If domain-wise losses under `poolPCA` vary substantially, this flags heterogeneity across domains that may warrant further investigation. If a worst-case solution differs substantially from `poolPCA`, it provides a principled alternative representation that explicitly trades-off a small reduction in average performance for improved worst-case behavior.

3 Robustness guarantees

3.1 Population guarantees

Optimizing any of the worst-case objectives described in Section 2.2 the following strong robustness guarantee: the solution remains worst-case optimal not only for the source domains but also for all distributions whose covariances lie in the convex hull of the (possibly normalized) source covariances. In contrast, standard approaches such as pooled or separate PCA do not offer such guarantees. The following two theorems summarize the results for all worst-case objectives from Section 2.2.

Theorem 6 (Robustness of wcPCA) *Consider Setting 1. Let*

$$\mathcal{C} := \text{conv}(\{\Sigma_e\}_{e \in \mathcal{E}}) \quad \text{and} \quad \mathcal{P} := \left\{ P \in \mathcal{P}(\mathbb{R}^p) \mid \mathbb{E}[\mathbf{x}] = 0, \mathbb{E}[\mathbf{x}^\top \mathbf{x}] \in \mathcal{C} \right\} \quad (4)$$

be the convex hull of the source covariances and the corresponding uncertainty set of distributions with zero mean and covariance in \mathcal{C} , respectively. Let $V_k^ \in \mathcal{O}_{p \times k}$ solve rank- k **maxRCS**, **minPCA**, or **maxRegret**. Let \mathcal{L} denote the corresponding loss function, i.e., $\mathcal{L} = \mathcal{L}_{\text{RCS}}$ for **maxRCS**, $\mathcal{L} = -\mathcal{L}_{\text{var}}$ for **minPCA**, and $\mathcal{L} = \mathcal{L}_{\text{reg}}$ for **maxRegret**. Then, the following statements hold.*

i) For all $V_k \in \mathcal{O}_{p \times k}$, the worst-case loss over \mathcal{P} equals the worst-case loss over the source domains, i.e.,

$$\sup_{P \in \mathcal{P}} \mathcal{L}(V_k; P) = \max_{e \in \mathcal{E}} \mathcal{L}(V_k; P_e).$$

ii) Consequently, the ordering induced by the worst-case loss over the source domains is preserved over \mathcal{P} : for all $V_k, W_k \in \mathcal{O}_{p \times k}$, if $\max_{e \in \mathcal{E}} \mathcal{L}(V_k; P_e) < \max_{e \in \mathcal{E}} \mathcal{L}(W_k; P_e)$, then $\sup_{P \in \mathcal{P}} \mathcal{L}(V_k; P) < \sup_{P \in \mathcal{P}} \mathcal{L}(W_k; P)$.

iii) Hence, V_k^ is worst-case optimal over \mathcal{P} , i.e., $V_k^* \in \arg \min_{V \in \mathcal{O}_{p \times k}} \sup_{P \in \mathcal{P}} \mathcal{L}(V; P)$.*

*iv) Statement iii) does not generally hold for the solutions to **poolPCA** and **sepPCA**.*

With a slight modification of the proof, one can show that Theorem 6 extends to the normalized objectives **norm-maxRCS**, **norm-minPCA**, and **norm-maxRegret** after modifying the uncertainty set.

Theorem 7 (Robustness of wcPCA, normalized) *Let $\mathcal{C}_{\text{norm}} := \text{conv}(\{\Sigma_e / \text{Tr}(\Sigma_e)\}_{e \in \mathcal{E}})$ and*

$$\mathcal{P}_{\text{norm}} := \left\{ P \in \mathcal{P}(\mathbb{R}^p) \mid \mathbb{E}_{\mathbf{x} \sim P}[\mathbf{x}] = 0, \frac{\mathbb{E}_{\mathbf{x} \sim P}[\mathbf{x}^\top \mathbf{x}]}{\mathbb{E}_{\mathbf{x} \sim P}[\|\mathbf{x}\|_2^2]} \in \mathcal{C}_{\text{norm}} \right\}. \quad (5)$$

Then the same statements as in Theorem 5 hold when replacing \mathcal{L} with $\mathcal{L}_{\text{normRCS}}$ (for reconstruction), $-\mathcal{L}_{\text{normVar}}$ (for variance), or $\mathcal{L}_{\text{normReg}}$ (for regret), and replacing \mathcal{P} with $\mathcal{P}_{\text{norm}}$.

Although similar in spirit, the results do not follow from Group DRO (Sagawa et al., 2020), as we outline in Appendix A.3.

3.2 Finite-sample guarantees and consistency

So far, we have focused on population-level objectives. We now prove analogous results in a finite-sample setting. Moreover, we prove that the empirical estimators are consistent for the population solutions and asymptotically worst-case optimal.

Setting 2 (Source domains, finite sample) *Consider Setting 1. For all $e \in \mathcal{E}$, let $X_e \in \mathbb{R}^{n_e \times p}$ be a data matrix of n_e i.i.d. observations from P_e . Define the empirical covariance as $\hat{\Sigma}_e := \frac{1}{n_e} X_e^\top X_e$. Let $n := \sum_{e \in \mathcal{E}} n_e$, $X_{\text{pool}} := [X_1^\top, \dots, X_E^\top]^\top \in \mathbb{R}^{n \times p}$ be the pooled data and $\hat{\Sigma}_{\text{pool}} := \frac{1}{n} X_{\text{pool}}^\top X_{\text{pool}}$ its covariance. We assume that for all $e \in \mathcal{E}$, $\text{Tr}(\hat{\Sigma}_e) > 0$.*

Given Setting 2, we define the empirical analogues of poolPCA and the worst-case PCA objectives. We say:

$$\begin{aligned} \hat{V}_k^{\text{pool}} \text{ solves rank-}k \text{ empirical poolPCA if } \hat{V}_k^{\text{pool}} &\in \arg \max_{V \in \mathcal{O}_{p \times k}} \text{Tr}(V^\top \hat{\Sigma}_{\text{pool}} V), \\ \hat{V}_k^{\text{minPCA}} \text{ solves rank-}k \text{ empirical minPCA if } \hat{V}_k^{\text{minPCA}} &\in \arg \max_{V \in \mathcal{O}_{p \times k}} \min_{e \in \mathcal{E}} \text{Tr}(V^\top \hat{\Sigma}_e V), \\ \hat{V}_k^{\text{maxRCS}} \text{ solves rank-}k \text{ empirical maxRCS if } \hat{V}_k^{\text{maxRCS}} &\in \arg \min_{V \in \mathcal{O}_{p \times k}} \max_{e \in \mathcal{E}} \frac{1}{n_e} \|X_e - X_e V V^\top\|_F^2. \end{aligned}$$

Analogous definitions of empirical maxRegret, norm-minPCA, norm-maxRCS, and norm-maxRegret are given in Appendix A.4.

Remark 8 *The empirical formulations exhibit optimality guarantees similar to their population counterparts when considering the convex hull of empirical covariance matrices rather than population covariances. More concretely, we provide a representative result in Appendix A.4, Proposition 17).*

We now prove that the worst-case estimators are asymptotically consistent for the population subspace (Proposition 9) and the worst-case guarantees of Theorem 6 hold asymptotically (Proposition 10). To establish these results, we require a uniqueness condition.

Assumption 1 *Each population problem maxRCS, norm-maxRCS, minPCA, norm-minPCA, maxRegret, and norm-maxRegret admits a unique solution up to right multiplication by an orthonormal matrix. That is, if V_k^* and \tilde{V}_k are both solutions, then there exists $Q \in \mathbb{R}^{k \times k}$ with $Q^\top Q = QQ^\top = I_k$ such that $V_k^* = \tilde{V}_k Q$, or, equivalently, $\text{span}(V_k^*) = \text{span}(\tilde{V}_k)$.*

Assumption 1 avoids set-valued limits (up to rotation). It holds under several conditions. For example, if a single domain strictly determines the worst-case loss at the optimum, the problem reduces to standard PCA on that domain, and Assumption 1 follows from a strict eigengap between the k -th and $(k+1)$ -th eigenvalue in the corresponding covariance matrix (normalized where applicable). In addition, if multiple domains are ‘active’ at the optimum, Assumption 1 holds if their (normalized) covariances share a common top- k eigenspace and each has a strict eigengap between its k -th and $(k+1)$ -th eigenvalue. In our simulations, Assumption 1 seems to hold. For example, repeating the experiment of Section 5.1.2 and solving the worst-case low-rank problem twice over 100 runs, the median projection distance (see Proposition 9) between the two solutions in each run is approximately 0.04, corresponding (if concentrated in one principal angle) to about 1.66° . Finally, we hypothesize that Propositions 9 and 10 hold more generally – even in (possibly non-generic) settings, where Assumption 1 is violated.

Proposition 9 (Consistency of the estimators) *Consider Setting 2. Let V_k^* and \hat{V}_k denote the population and empirical solutions, respectively, to maxRCS, norm-maxRCS, minPCA, norm-minPCA, maxRegret, or norm-maxRegret, and let $n_{\min} := \min_{e \in \mathcal{E}} n_e$. Under Assumption 1, as $n_{\min} \rightarrow \infty$, we have*

$$d(\hat{V}_k, V_k^*) \xrightarrow{P} 0$$

where $d(V_1, V_2) := \|V_1 V_1^\top - V_2 V_2^\top\|_F$ and \xrightarrow{P} denotes convergence in probability.

We further show that the empirical solutions are asymptotically worst-case optimal, in the sense of Theorem 6. First, the empirical estimator achieves the optimal worst-case population loss in the limit. Second, the empirical objective provides an asymptotic upper bound on the population loss over all distributions in the uncertainty set.

Proposition 10 (Asymptotic worst-case optimality) *Consider Setting 2. Let \hat{V}_k and V_k^* be the empirical and population solutions, respectively, to $\max\text{RCS}$, norm-maxRCS , $\min\text{PCA}$, norm-minPCA , $\max\text{Regret}$, or norm-maxRegret . Let \mathcal{L} denote the corresponding loss⁴ and let \mathcal{Q} denote the associated distributional class (\mathcal{P} for the unnormalized losses, $\mathcal{P}_{\text{norm}}$ for the normalized losses). Under Assumption 1, as $n_{\min} := \min_{e \in \mathcal{E}} n_e \rightarrow \infty$, the following two statements hold.*

i) *The worst-case population loss of \hat{V}_k converges in probability to the optimal value,*

$$\sup_{P \in \mathcal{Q}} \mathcal{L}(\hat{V}_k; P) \xrightarrow{P} \sup_{P \in \mathcal{Q}} \mathcal{L}(V_k^*; P).$$

ii) *For every $\epsilon > 0$,*

$$\lim_{n_{\min} \rightarrow \infty} \Pr \left(\sup_{P \in \mathcal{Q}} \mathcal{L}(\hat{V}_k; P) > \hat{m}_k + \epsilon \right) = 0,$$

where $\hat{m}_k := \max_{e \in \mathcal{E}} \mathcal{L}(\hat{V}_k; \hat{\Sigma}_e)$ is the empirical loss⁵.

Here, ii) does not follow directly from finite-sample robustness, see Remark 8, because the distribution class \mathcal{Q} is formed from the population not the empirical covariance matrices.

4 Extension: worst-case matrix completion

When data are only partially observed, low rank approximation extends naturally to matrix completion. In the single-domain setting, a common formulation (e.g., Jain et al., 2013) approximates $X \in \mathbb{R}^{n \times p}$ by a rank- k factorization $X \approx LR^\top$, where $L \in \mathbb{R}^{n \times k}$ and $R \in \mathbb{R}^{p \times k}$ (with $k \ll p$), by minimizing reconstruction error over the observed entries. A classic example is movie recommendation (e.g., Harper and Konstan, 2015), where rows correspond to users and columns to movies. Only a subset of ratings is observed, and the goal is to predict the missing entries under a low-rank assumption. The factorization can be interpreted as modeling latent features (e.g., genre or style) that explain preferences: the left factor represents user-specific weights on these features, while the right factor encodes the weights of the movies.

As before, the data may arise from multiple domains. In the movie example, this occurs when users belong to heterogeneous subpopulations (e.g., regions or age groups) with differing rating patterns. We now extend the worst-case framework developed for PCA to matrix completion. In particular, we introduce a worst-case objective for multi-domain matrix completion and formalize inductive matrix completion in target domains.

4. So $\mathcal{L} \in \{-\mathcal{L}_{\text{var}}, -\mathcal{L}_{\text{normVar}}, \mathcal{L}_{\text{RCS}}, \mathcal{L}_{\text{normRCS}}, \mathcal{L}_{\text{reg}}, \mathcal{L}_{\text{normReg}}\}$, as in Theorems 6 and 7.

5. In Equation (2) and (3) we define the losses \mathcal{L} as a function of the distribution P . Each loss depends on the distribution P only through its covariance matrix Σ , so, by slight abuse of notation, we can write the losses in terms of Σ . For example, for all $V \in \mathcal{O}_{p \times k}$, $\mathcal{L}_{\text{RCS}}(V; P) = \mathcal{L}_{\text{RCS}}(V; \Sigma) := \text{Tr}(\Sigma) - \text{Tr}(V^\top \Sigma V)$.

We then show the following worst-case optimality guarantee: when the source domains are fully observed but the target domains incur missingness, subspaces that are worst-case optimal for reconstruction error remain ϵ -worst-case optimal over the convex hull of the source covariances.

Setting 3 (Multiple domains with missingness) Consider Setting 1. For each domain $e \in \mathcal{E}$, the entries of $\mathbf{x}_e \in \mathbb{R}^p$ are observed according to a mask $\omega_e \in \{0, 1\}^p$, where ω_e is drawn independently of \mathbf{x}_e from a distribution Q : $(\omega_e)_i = 1$ if the i -th entry of \mathbf{x}_e is observed and $(\omega_e)_i = 0$ otherwise

Setting 4 (Finite-sample version) Consider Setting 3. For each $e \in \mathcal{E}$, let $X_e \in \mathbb{R}^{n_e \times p}$ be a data matrix of n_e i.i.d. rows from P_e , and let $\Omega_e \in \{0, 1\}^{n_e \times p}$ contain n_e masks drawn i.i.d. from Q ; only entries with $(\Omega_e)_{ij} = 1$ are observed. Let $n := \sum_{e \in \mathcal{E}} n_e$ and $X_{\text{pool}} \in \mathbb{R}^{n \times p}$ and $\Omega_{\text{pool}} \in \{0, 1\}^{n \times p}$ denote the row-wise concatenation of the domain-specific matrices.

In the multi-domain setting, a natural baseline is to ignore domain labels and solve matrix completion on the pooled data $(X_{\text{pool}}, \Omega_{\text{pool}})$, minimizing average reconstruction error across domains; we term this solving `poolMC`. Similarly as for `wcPCA`, we can also optimize the worst-case reconstruction error.

Definition 11 (maxMC) Consider Setting 4. A (shared) right factor $R^* \in \mathbb{R}^{p \times k}$ and (domain-specific) left factors $L_e^* \in \mathbb{R}^{n_e \times k}$ for $e \in \mathcal{E}$ solve `maxMC` if

$$(R^*, L_1^*, \dots, L_E^*) \in \arg \min_{\substack{R \in \mathcal{O}_{p \times k} \\ \forall e \in \mathcal{E}, L_e \in \mathbb{R}^{n_e \times k}}} \max_{e \in \mathcal{E}} \frac{1}{n_e} \|P_{\Omega_e}(X_e) - P_{\Omega_e}(L_e R^\top)\|_F^2, \quad (6)$$

where, for all $e \in \mathcal{E}$, $P_{\Omega_e} : \mathbb{R}^{n_e \times p} \rightarrow \mathbb{R}^{n_e \times p}$ is defined as $[P_{\Omega_e}(X_e)]_{ij} = [X_e]_{ij}$ if $(\Omega_e)_{ij} = 1$ and $[P_{\Omega_e}(X_e)]_{ij} = 0$ otherwise.

This objective learns a shared right factor that minimizes worst-case reconstruction error across domains. In the single-domain setting, this coincides with the standard matrix completion objective. Additionally, in absence of missingness in the source domains, the shared right factor that solves `maxMC` coincides with the solution to empirical `maxRCS`, since P_{Ω_e} reduces to the identity and, for all $e \in \mathcal{E}$, the optimal choice of L_e is $L_e = X_e R$.

4.1 Inductive matrix completion

After learning a shared right factor R^* on the source domains, we can also use it to reconstruct new, partially observed observations in a target domain (in the movie recommendation example, this could correspond to new users in a new domain) – a problem that is sometimes referred to as inductive matrix completion. We can, for example, reconstruct a row $\mathbf{x} \in \mathbb{R}^{1 \times p}$ observed on coordinates ω , by estimating coefficients $\ell \in \mathbb{R}^k$ from the observed entries and forming $\hat{\mathbf{x}} = \ell(R^*)^\top$. In this paper, we focus on the ordinary least squares estimator,

$$\ell_{\text{OLS}} = \ell_{\text{OLS}}(\mathbf{x}, \omega, R^*) \in \arg \min_{\ell \in \mathbb{R}^k} \sum_{i \in [p]: \omega_i = 1} (\mathbf{x}_i - [\ell(R^*)^\top]_i)^2, \quad (7)$$

an approach that is commonly used (e.g., Koren et al., 2009); alternative methods such as incorporating side information (e.g., Jain and Dhillon, 2013) could also be considered.

4.2 Robustness guarantees

We consider the setting in which the source domains are fully observed and missingness arises only in the target domain. In this setting, we prove that a subspace that is worst-case optimal for reconstruction remains ϵ -worst-case optimal for inductive matrix completion over the convex hull of the source covariances. We impose incoherence of the right factor—a standard assumption in matrix completion—and require a minimum number of observed entries; later, this allows us to control the reconstruction error under missingness.

Definition 12 (μ -incoherence) *Let $R \in \mathcal{O}_{p \times k}$. We say that R is μ -incoherent if, for all $i \in [p]$, $\|R^{(i)}\|_2 \leq \mu \sqrt{\frac{k}{p}}$, where $R^{(i)}$ denotes the i -th row of R .*

Assumption 2 (Sufficient observations) *Let $\epsilon \in (0, 1)$ and $\mu \geq 1$. For $\omega \sim Q$, the number of unobserved entries s satisfies $s \leq \frac{p\epsilon}{k\mu^2(2\epsilon+1)}$ almost surely.*

As in Theorem 6, let \mathcal{C} be the convex hull of the domain covariance matrices and let \mathcal{P} denote the set of distributions with covariance in \mathcal{C} . Additionally, for all distributions P, Q over \mathbf{x} and ω , for all $R \in \mathcal{O}_{p \times k}$, let $\mathcal{L}_{P, Q}(R) := \mathbb{E}_{\mathbf{x} \sim P, \omega \sim Q} \|\mathbf{x} - \ell_{\text{OLS}}(\mathbf{x}, \omega, R)R^\top\|_2^2$ be the expected reconstruction error of $\mathbf{x} \sim P$ under sampling distribution Q .

Theorem 13 (Worst-case robustness for inductive completion) *Consider Setting 3 and let $\epsilon \in (0, 1)$. Assume the source domains are fully observed, i.e., the source mask distribution Q_{source} satisfies $Q_{\text{source}}(\omega = \mathbf{1}) = 1$. Let $R^* \in \mathcal{O}_{p \times k}$ solve the population worst-case matrix completion problem, defined as*

$$R^* \in \arg \min_{R \in \mathcal{O}_{p \times k}} \max_{e \in \mathcal{E}} \mathcal{L}_{P_e, Q_{\text{source}}}(R). \quad (8)$$

(R^ thus also solves maxRCS .) Let Q_{target} be the distribution of the masks in the target domains. If R^* is μ -incoherent, and Assumption 2 holds for Q_{target} with this μ , then R^* is ϵ -worst-case optimal for inductive matrix completion over \mathcal{P} , that is,*

$$\sup_{P \in \mathcal{P}} \mathcal{L}_{P, Q_{\text{target}}}(R^*) \leq (1 + \epsilon) \min_{R \in \mathcal{O}_{p \times k}} \sup_{P \in \mathcal{P}} \mathcal{L}_{P, Q_{\text{target}}}(R).$$

Thus, a subspace that is worst-case optimal for low-rank approximation remains (approximately) worst-case optimal for inductive matrix completion over all distributions in \mathcal{P} . Theorem 13 analyzes the regime in which the source domains are fully observed (so that maxMC reduces to maxRCS). Our simulations indicate that, even when the source domains are only partially observed, maxMC improves worst-case reconstruction error relative to poolMC (see Section 5.2). Furthermore, the bound on the number of unobserved entries imposed by Assumption 2 is restrictive (e.g., for $(k, \epsilon, \mu) = (2, 0.1, 1)$, the bound yields $s \leq 0.0417p$, i.e., approximately 4% missing entries). Nevertheless, empirically, robustness degrades only mildly as missingness increases, and maxMC continues to outperform pooling well beyond the guaranteed regime (see Section 5.2). We thus believe that stronger versions of Theorem 13 may hold.

5 Numerical experiments

We investigate the worst-case estimators through synthetic simulations. In each experiment, we consider five source domains, obtained by sampling five population covariance matrices $(\Sigma_1, \dots, \Sigma_e)$ in $\mathbb{R}^{p \times p}$ ($p = 20$ unless otherwise stated) of rank 10 from a measure $\mathbb{Q}_{\alpha, \beta}$ that depends on parameters α, β (the role and standard choices of the parameters are explained in Appendix B.1); in each experiment we resample the covariance matrices. Under the measures $\mathbb{Q}_{\alpha, \beta}$, the sampled covariances consist of a rank-5 shared component and a rank-5 domain-specific component with shared eigenvalues across domains, and are trace-normalized. These properties ensure that the solutions to `minPCA`, `maxRCS`, `maxRegret`, and their normalized variants all coincide. We therefore report only the results of `maxRCS` and evaluate performance using reconstruction error. The only exception is Section 5.1.4, where we modify the data-generating process to study the effect of heterogeneous noise. Appendix B.1 provides more details on the data generating process. The `wcPCA` variants are solved using projected gradient descent (Appendix B.2 provides further details including a comparison of our implementation to the approximations of Wang et al. (2025) and Tantipongpipat et al. (2019)) and `poolMC` and `maxMC` are solved with alternating minimization (also see Appendix B.2). Code to reproduce all simulations and figures is publicly available at <https://github.com/anyafries/wcPCA>.

5.1 Worst-case low-rank approximation

5.1.1 CONVEX-HULL ROBUSTNESS IN THE POPULATION CASE

We illustrate Theorem 6(i) stating that, for `maxRCS`, the maximum reconstruction error on the source domains provides a minimal upper bound for the reconstruction error of all covariances in their convex hull. To do so, we sample five source covariances $\mathcal{C}_{\text{source}} := (\Sigma_1, \dots, \Sigma_5) \sim \mathbb{Q}_{\alpha, \beta}$ and compute the rank-5 population solutions to `poolPCA` and `maxRCS`, V^{pool} and V^{maxRCS} . We sample 50 target covariances, collected in the set $\mathcal{C}_{\text{target}}$, from the convex hull of the source covariances (as described in Appendix B.1). For every $\Sigma \in \mathcal{C}_{\text{target}} \cup \mathcal{C}_{\text{source}}$, we compute the reconstruction errors using `poolPCA` and `maxRCS`, that is, $\mathcal{L}_{\text{RCS}}(V^{\text{pool}}; \Sigma)$ and $\mathcal{L}_{\text{RCS}}(V^{\text{maxRCS}}; \Sigma)$. Figure 3 shows that all test errors of `maxRCS` lie below the bound $m_{\text{maxRCS}}^* := \max_{1 \leq e \leq 5} \mathcal{L}_{\text{RCS}}(V^{\text{maxRCS}}; \Sigma_e)$, as guaranteed by Theorem 6(i). In contrast, `poolPCA` exceeds this bound in several cases.

5.1.2 AVERAGE VERSUS WORST-CASE PERFORMANCE

We next study how much average performance `maxRCS` loses in exchange for improved worst-case robustness compared to `poolPCA`. We vary the heterogeneity between domains by varying the parameters α, β in the distribution of the source covariances $\mathbb{Q}_{\alpha, \beta}$ (see Appendix B.1 for more details); we consider $(\alpha, \beta) \in \{(0.1, 0.5), (0.5, 1), (1, 2), (2, 5)\}$. Higher values of (α, β) increase the contribution of domain-specific components, creating greater variation between domains. For each (α, β) , we repeat the following steps 25 times. We sample $(\Sigma_1, \dots, \Sigma_5) \sim \mathbb{Q}_{\alpha, \beta}$, compute rank-5 solutions V^{pool} and V^{maxRCS} , and report the difference in average reconstruction error (over the source domains) and worst-case reconstruction error (over the convex hull of the source covariances), relative to the average performance of `poolPCA` (for details, see equations (10) and (11) in Appendix B.3). The

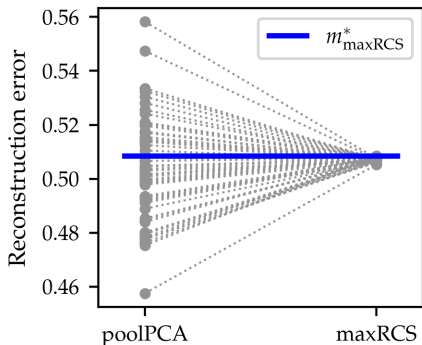


Figure 3: *Illustration of Theorem 6(i); see Section 5.1.1.* Reconstruction errors for the source domains and 50 target domains are shown for `poolPCA` and `maxRCS` in a population setting. The blue line marks m_{maxRCS}^* , the maximum reconstruction error over the source domains. As expected from Theorem 6(i), all `maxRCS` errors lie below this bound, whereas `poolPCA` exceeds it in several cases.

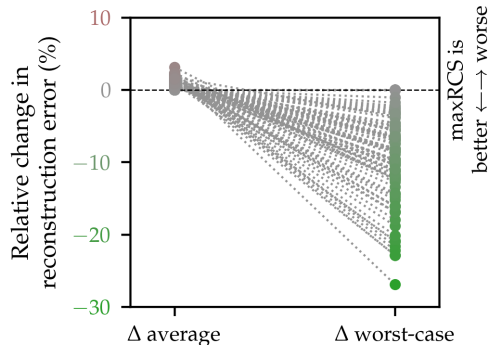


Figure 4: *Average vs. worst-case reconstruction error of `maxRCS` and `poolPCA`; see Section 5.1.2.* The difference in errors are shown relative to `poolPCA`’s average performance. Values below zero indicate that `maxRCS` outperforms `poolPCA`. `maxRCS` improves worst-case performance, while incurring only small losses on average.

results are shown in Figure 4. Solutions to `maxRCS` consistently improve worst-case error while incurring only small losses in average error, across varying domain heterogeneity. These findings complement Theorem 6(iii): while the theorem guarantees that there exist settings where `maxRCS` strictly outperforms `poolPCA` in the worst case, the simulations suggest that such improvements occur generically.

5.1.3 CONVERGENCE AND FINITE-SAMPLE ROBUSTNESS

Proposition 10(i) states that the worst-case population loss of the empirical `maxRCS` solution converges in probability to the optimal worst-case population loss. We illustrate this convergence empirically and additionally assess the finite-sample robustness of `maxRCS` relative to pooled PCA. To do so, we vary the sample size $n \in \{100, 250, 500, 1000, 2000, 5000\}$ and heterogeneity (α, β) as in Section 5.1.2. For each (n, α, β) we repeat the following steps 25 times. We sample source covariances $\mathcal{C}_{\text{source}} := (\Sigma_1, \dots, \Sigma_5) \sim \mathbb{Q}_{\alpha, \beta}$ and, for all domains $1 \leq e \leq 5$, we draw n observations from $\mathcal{N}(0, \Sigma_e)$, and compute the rank-5 empirical and population solutions of `poolPCA` and `maxRCS`, denoted as $\hat{V}^{\text{pool}}, \hat{V}^{\text{maxRCS}}, V^{\text{pool}}$, and V^{maxRCS} , respectively.

We assess convergence by reporting the difference in worst-case population reconstruction error (evaluated over the convex hull $\text{conv}(\mathcal{C}_{\text{source}})$) between empirical and population `maxRCS` (for details, see equation (12) in Appendix B.3). Values near zero indicate that the empirical estimator attains nearly optimal worst-case performance over the convex hull of the population matrices. Figure 5 (left) illustrates behavior in line with Proposition 10(i),

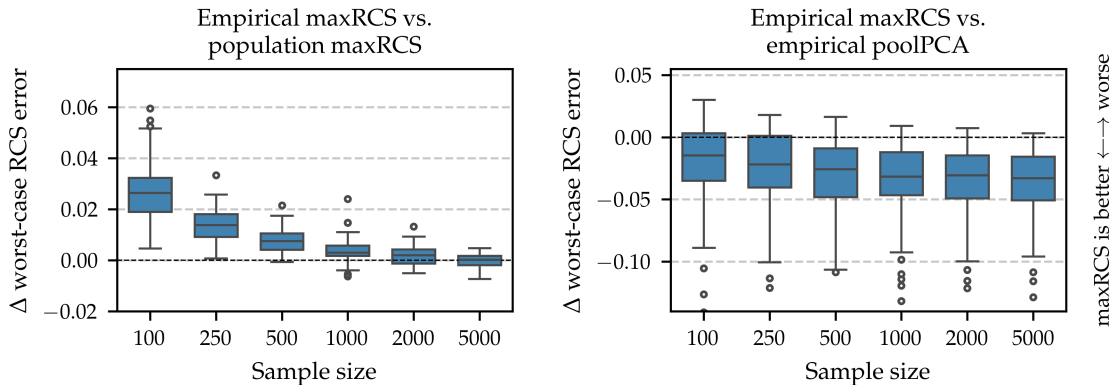


Figure 5: *Finite-sample performance of maxRCS*; see Section 5.1.3. *Left*: Difference in worst-case loss (reconstruction error) over the convex hull of the population covariance matrices between empirical and population maxRCS. *Right*: Analogous difference between empirical maxRCS and empirical poolPCA. Negative values indicate that maxRCS attains lower worst-case error than poolPCA. Across sample sizes, maxRCS outperforms poolPCA.

with the distribution of the difference increasingly concentrated around zero as n increases.

In the same way, we also compare empirical maxRCS and empirical poolPCA (for details, see equation (13) in Appendix B.3). Figure 5 (right) shows that maxRCS outperforms poolPCA across sample sizes, showing that the practical benefits of maxRCS may emerge even at modest sample sizes.

5.1.4 USING REGRET AS A PROXY FOR RECONSTRUCTION ERROR UNDER HETEROGENEOUS NOISE

This experiment shows that, under heterogeneous noise across domains, worst-case regret may outperform worst-case reconstruction- or variance-based objectives, even when evaluated using reconstruction error, consistent with the discussion in Section 2.2.6. We again sample five source covariances $\Sigma_1, \dots, \Sigma_5$, as described in Appendix B.1, using the variant in which the domain-specific eigenvalues differ across domains. Then, for all domains $e \in \mathcal{E}$, we draw a noise level $\sigma_e \sim U([0, 0.1])$ and sample $n = 2000$ i.i.d. training observations according to

$$\mathbf{z}_e = \mathbf{x}_e + \sigma_e \boldsymbol{\varepsilon}_e, \quad \mathbf{x}_e \sim \mathcal{N}(0, \Sigma_e), \quad \boldsymbol{\varepsilon}_e \sim \mathcal{N}(0, I_p);$$

thus, the population covariance is $\Sigma_e + \sigma_e^2 I_p$. We solve rank-10 and rank-5 maxRCS and maxRegret⁶ using the empirical covariances, and evaluate both methods in terms of worst-case reconstruction error on n independent observations from $\mathcal{N}(0, \Sigma_e)$ without additional heterogeneous noise. The experiment is repeated 25 times and results are shown in Figure 6.

6. As the domain-specific eigenvalues vary between domains, the solutions to maxRCS and maxRegret no longer necessarily coincide. However, all covariances are trace-normalized, so the solutions to minPCA, maxRCS, and their normalized variants all coincide, and we report results only for maxRCS. Likewise, the solutions to maxRegret and norm-maxRegret coincide, and we report results only for maxRegret.

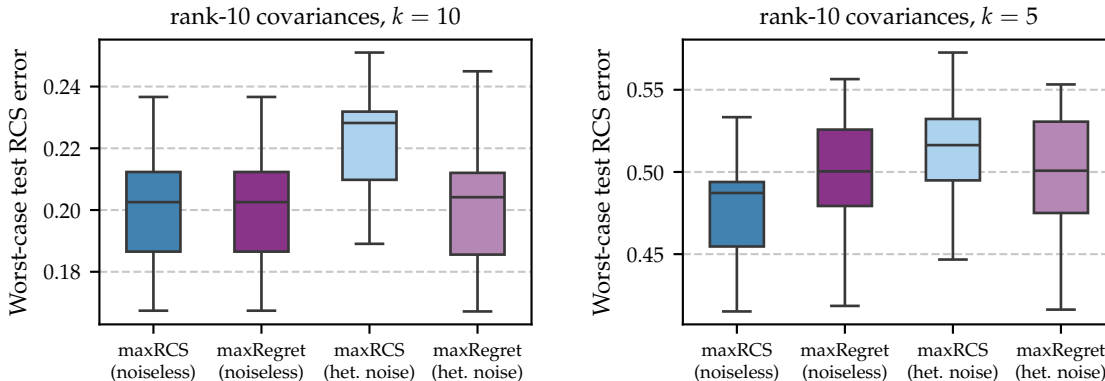


Figure 6: *Regret may be preferable under heterogeneous noise; see Section 5.1.4.* *Left:* As suggested by the population theory, solutions to `maxRCS` and `maxRegret` are almost identical in the noiseless case. With heterogeneous noise, `maxRegret` behaves similarly as if the data were noiseless. *Right:* When k is strictly smaller than the rank of the covariance matrices, solutions to `maxRCS` and `maxRegret` differ in the noiseless case. Nevertheless, under heterogeneous noise, `maxRegret` can still be preferable over `maxRCS` even if the evaluation criteria is reconstruction error.

When the approximation rank k matches the rank of the covariances (rank 10), the solutions of `maxRegret` and `maxRCS` coincide in the noiseless population case and the population solution of `maxRegret` is insensitive to heterogeneous noise (see Section 2.2.6 for both statements) For finitely many observations, these equalities do not hold exactly. Nevertheless, Figure 6 (left) illustrates empirical behavior consistent with the population theory: in the noiseless case, `maxRCS` and `maxRegret` yield similar worst-case reconstruction errors, and under heterogeneous noise, `maxRegret` approximately recovers the solution obtained in the noiseless case, whereas `maxRCS` incurs increased worst-case reconstruction error. When using a lower-rank approximation ($k = 5$), the population solution of `maxRegret` is still unaffected by heterogeneous noise (see Section 2.2.6), but those of `maxRegret` and `maxRCS` no longer coincide (see, e.g., Example 1). Figure 6 (right) shows similar empirical results: in the noiseless case, `maxRCS` and `maxRegret` differ, and under heterogeneous noise, `maxRegret` exhibits similar behavior while `maxRCS` incurs higher worst-case reconstruction error. These results indicate that regret-based objectives may be preferable under heterogeneous noise, even when the goal is robust reconstruction.

5.2 Worst-case inductive matrix completion

We study worst-case matrix completion in two regimes: (i) fully observed source domains (the setting of Theorem 13), and (ii) partially observed source domains. Our simulations show that `maxMC` generally reduces worst-case reconstruction error relative to `poolMC`, including when source domains are partially observed and missingness exceeds the theoretical bound.

As in Section 5.1.2, we vary domain heterogeneity, which is controlled by (α, β) . For each configuration, we repeat the following steps 25 times. We sample five rank-10 source

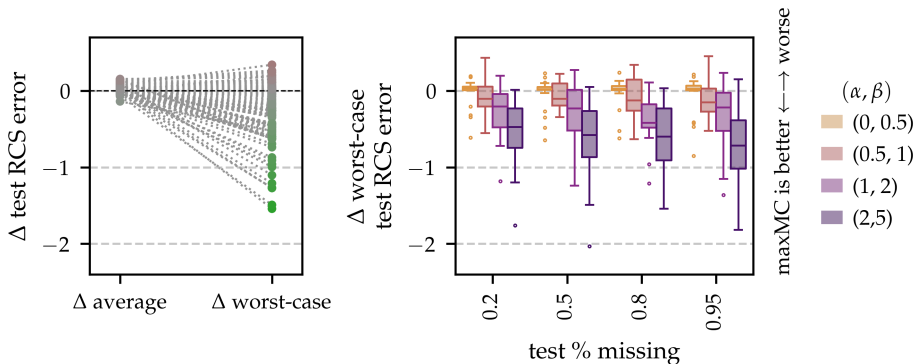


Figure 7: *Worst-case inductive matrix completion with partially observed source domains (90% missing entries; regime (ii)).* *Left:* Difference in average and worst-case test reconstruction error between maxMC and poolMC . In line with Theorem 13 (which covers the population case and allows for some ϵ deviation), maxMC generally improves worst-case performance; in terms of average error, it incurs only minor changes. *Right:* Worst-case difference as the proportion of missing target entries varies, for different heterogeneity levels (α, β) . maxMC achieves lower median worst-case error than poolMC , with larger gains under stronger domain heterogeneity.

covariances $(\Sigma_1, \dots, \Sigma_5) \sim \mathbb{Q}_{\alpha, \beta}$ with dimension $p = 500$ and, for all domains $1 \leq e \leq 5$, we draw $n = 1000$ observations from $\mathcal{N}(0, \Sigma_e)$. In regime (i), source data are fully observed; in regime (ii), 90% of entries in each source row are selected uniformly at random and masked. In each regime, we learn shared right factors via poolMC and maxMC . For evaluation, we draw 1000 independent test observations per domain and mask 90% of entries uniformly at random. Reconstruction is performed using the least-squares rule of Section 4.1. Performance is measured by per-entry mean squared reconstruction error, either averaged across domains or in the worst-case domain (see Appendix B.3 for details).

Figure 7 shows the results of the more difficult regime (ii); the left panel shows that maxMC generally reduces worst-case target reconstruction error relative to pooling while incurring only small changes in average performance. The right panel varies the proportion of missing target entries and shows that, under high domain heterogeneity, the worst-case advantage of maxMC persists even when substantially more entries are missing than specified by Assumption 2. Under low heterogeneity, performance is comparable to poolMC , reflecting the reduced variation across domains. Results for the simpler regime (i) are qualitatively similar and are shown in Figure B.iii in Appendix B.4.

6 Applications

6.1 Explaining variance in held-out FLUXNET regions

We illustrate the benefits of worst-case PCA objectives on FLUXNET data (Pastorello et al., 2020; Baldocchi, 2008). These data contain measurements of variables related to biosphere and atmosphere interactions obtained at different places on the Earth (see Figure 8

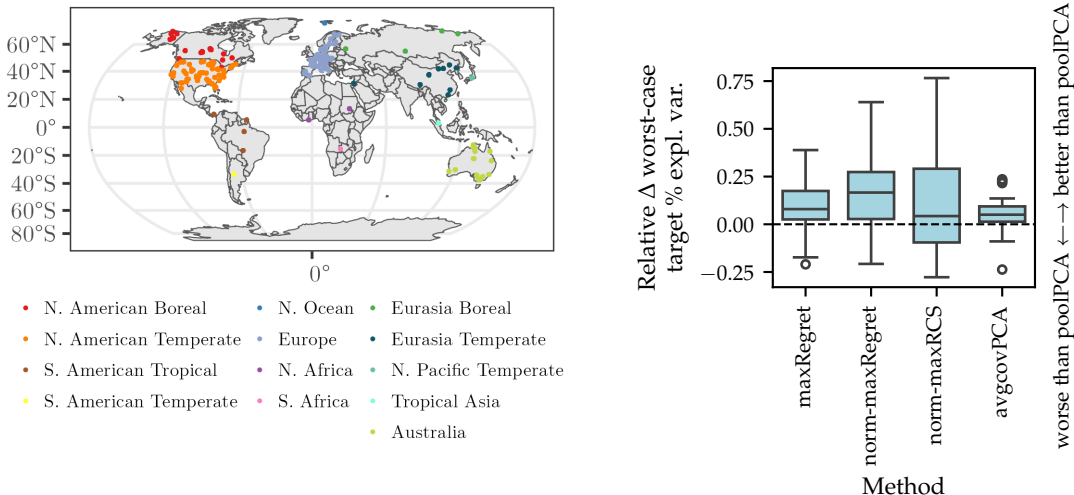


Figure 8: *Left*: Map of FLUXNET sites, colored by TransCom region. *Right*: Relative difference in worst-case proportion of explained variance between `poolPCA` and `maxRegret`, `norm-maxRegret`, `norm-maxRCS`, and `avgcovPCA`, evaluated on held-out target regions over 20 random train–test splits. Positive values indicate improved worst-case performance relative to pooled PCA. The worst-case objectives generally improve robustness, with `norm-maxRegret` achieving the strongest gains in median worst-case proportion of explained variance.

left). More precisely the variables comprise gross primary productivity (GPP), meteorological variables (air temperature, vapor pressure deficit, and day and night land surface temperature), and remote-sensing indices (EVI, NDVI, NDWI, LAI, NIRv, and fPAR). We group the data into TransCom regions (Gurney et al., 2004) as domains (see Figure 8, left), which spans heterogeneous climates and measurement conditions. The data pre-processing is described in Appendix C.1. Based on scree plots and the Kaiser criterion (Appendix C.1, Figure C.i), we consider rank-2 approximations to the data.

We perform 20 random splits of the regions into five source regions and eight target regions. On each split, we solve rank-2 `poolPCA`, `maxRegret`, `norm-maxRegret`, and `norm-minPCA` on the source regions. This setting extends the illustrative example in Section 1, where we compared `poolPCA` and `norm-maxRegret` on a single split of the TransCom regions. We use the normalized and regret-based variants because the total variance in each domain varies (see Section 2.2.6). For comparison, we solve rank-2 PCA on the average empirical covariance ($\frac{1}{|\mathcal{E}|} \sum_{e \in \mathcal{E}} \hat{\Sigma}_e$), denoted `avgcovPCA`, which removes the effect of unequal sample sizes across regions; to the best of our knowledge, it does not come with any extrapolation guarantee.

Figure 8 (right) reports the relative difference in worst-case proportion of explained variance between `poolPCA` and the other methods over the target regions (results for additional components are reported in Appendix C.1, Figure C.ii.). Positive values indicate improved worst-case performance relative to `poolPCA`. All alternatives to `poolPCA` improve worst-case performance on the target regions, including PCA on the average covariance. However, the

worst-case objectives typically perform best: **norm-maxRegret** achieves the strongest gains and improves worst-case explained variance in 16 out of 20 splits (p-value of a binomial test equals ca. 0.01) and a median improvement of 0.07 in absolute worst-case proportion of explained variance.

6.2 Reanalysis of the three major axes of terrestrial ecosystem function

We now revisit part of the analysis conducted by Migliavacca et al. (2021). The authors aggregate FLUXNET data over time to derive site-level functional ecosystem properties related to carbon uptake and release, energy and water exchange, and growing-season water-use efficiency (see Table 2 in Appendix C.2). Motivated, for example, by the task of predicting ecosystem responses to climatic changes, the authors sought a low-dimensional representation of ecosystem functioning, defining three axes of variation of terrestrial ecosystem function via PCA on the pooled dataset. Based on the loadings, these three axes are then interpreted to represent “maximum ecosystem productivity”, “ecosystem water-use strategies”, and “ecosystem carbon-use efficiency” (Migliavacca et al., 2021).

Arguably, such interpretations should be consistent over different continents. We thus evaluate the robustness of the three axes, when treating continents as distinct domains. We compare **poolPCA** (which corresponds⁷ to the analysis by Migliavacca et al. (2021)) against **norm-maxRCS** and **norm-maxRegret**, which explicitly optimize for worst-case performance across domains. (We use the normalized variants because total variance differs across continents, see Section 2.2.6; for completeness, results for PCA based on the average empirical covariance and for **maxRegret** are reported in Appendix C.2.)

Figure 9 compares the pooled and worst-case solutions. For **poolPCA**, we observe a substantial gap between the average in-sample proportion of explained variance and the worst-case performance across continents. In contrast, **norm-maxRCS** achieves nearly identical average proportion of explained variance while substantially improving worst-case performance. **norm-maxRegret** shows a similar, though smaller, improvement.

We further compare the loadings of **poolPCA** and **norm-maxRCS** (Figure 9, right), providing a diagnostic for whether the identified axes reflect domain-invariant ecological structure (Appendix A.2 details the construction of the ordered worst-case basis). The leading axis remains largely stable, reflecting maximum ecosystem productivity and its coupling with ecosystem respiration. The second axis may still be interpreted as a water-use strategy gradient dominated by the same six metrics, however, **norm-maxRCS** reduces the influence of the water use efficiency (WUE) loadings in favor of the remaining properties. The third axis, originally interpreted as carbon-use efficiency (aCUE, R_b , $R_{b_{\max}}$, EF_{ampl}), shifts most prominently: EF_{ampl} is effectively removed while G_1 and GS_{max} are upweighted, indicating a stronger contribution of water-regulation traits. In our view, the stability of the first two axes under worst-case optimization strengthens the interpretation of these axes as fundamental ecological gradients; our results also suggest that the interpretation of the third axis may warrant further investigation.

7. Here, we pre-process the data similarly to Section 6.1, which deviates slightly from the procedure used by Migliavacca et al. (2021). The differences are minor: for example, the loadings from **poolPCA** shown in Figure 9 are almost identical to those presented by Migliavacca et al. (2021). All details on pre-processing are provided in Appendix C.2.

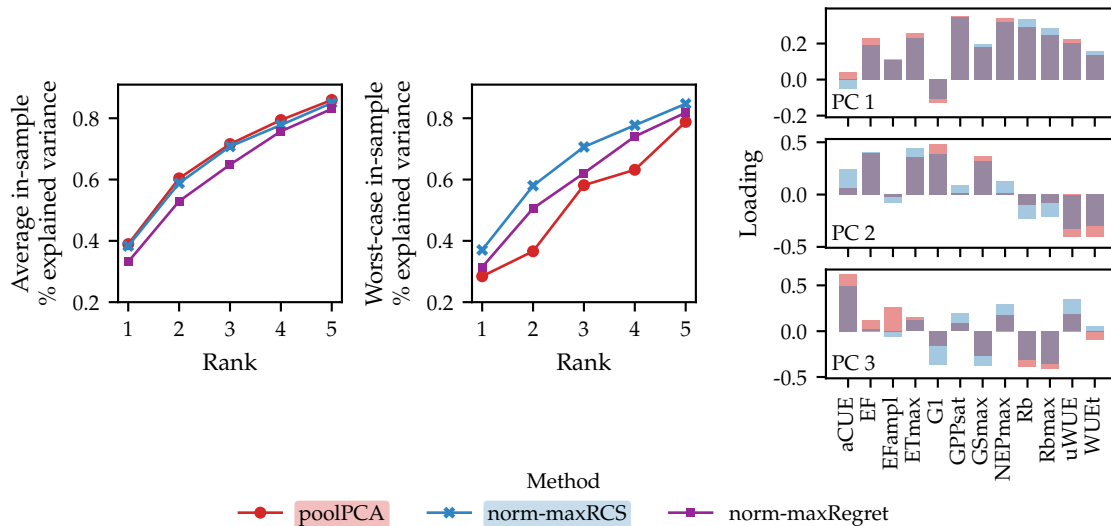


Figure 9: Comparison of dimensionality reduction methods on ecosystem function data across continents. *Left*: Proportion of variance explained on the pooled dataset. *Centre*: Worst-case proportion of variance explained across continents. *Right*: Loadings of the top three principal components for `poolPCA` and `norm-maxRCS`. `norm-maxRCS` improves worst-case proportion of explained variance with negligible loss in average performance, while largely retaining the physical interpretability of the principal axes.

7 Discussion

This paper studies worst-case formulations of low-rank approximation across multiple domains. Considering the worst-case instead of average-case can substantially improve performance in new target domains. The key theoretical guarantee is out-of-sample worst-case optimality over the convex hull of the source covariances (or of their normalized versions). Empirically, these objectives improve worst-case performance with only modest losses on average, as shown both on simulated data and case studies using real-world FLUXNET data.

The different worst-case objectives are not interchangeable. Normalized objectives mitigate sensitivity to scale differences by measuring proportional explained variance (or normalized reconstruction error), but unit comparability across domains is lost. Because worst-case objectives depend on ‘extreme’ domains, noisy or small domains can affect their solutions; the extent of this effect depends on the chosen objective. Normalization and the use of the regret can mitigate these effects to some extent. In particular, regret-based objectives evaluate performance relative to each domains’ optimal subspace and are robust to heterogeneous noise. On real data, we found that regret performs best even when the objective is explained variance or reconstruction error.

As in classical PCA, pre-processing choices (such as centering, scaling, standardization) matter. These choices can change which domain is worst-case and therefore change the solution. An additional choice is whether to form the pooled covariance from pooled data

or to average the domain covariances (these coincide when domain sample sizes are equal). While averaging can reduce the influence of large domains, as far as we know, it does not come with comparable out-of-sample guarantees.

When data are only partially observed, low-rank approximation can be used to tackle matrix completion. In the fully observed training regime, our convex-hull robustness guarantee transfers to inductive completion (up to an approximation factor). When source domains are also partially observed, `maxMC` remains empirically effective but our theory does not yet cover this setting; extending the out-of-sample guarantees to jointly handle domain heterogeneity and missingness in the source domains is left to future work. An additional direction is to allow domain-dependent observation mechanisms and to improve the bounds we establish

We regard the following additional extensions to be particularly promising. First, worst-case objectives can be used for nonlinear representation learning (e.g., autoencoders) by replacing the reconstruction loss with an appropriate domain-wise worst-case criterion. Second, robustness to distribution shift can be combined with robustness to corruption and outliers by integrating worst-case domain objectives with robust (in the sense of robustness against outliers) PCA-type modeling. Third, it is natural to consider interpolations between the pooled and worst-case objectives that trade average and worst-case performance, for instance via convex combinations or regularized formulations. Solutions to these objectives may provide smoother behavior when the worst-case domain is small or noisy, without discarding the robustness perspective. Fourth, when taking the diagnostics perspective, see Section 2.2.6, in settings where domains are ordered (e.g., through time), tracking domain-wise losses can be used to detect distribution shifts; for worst-case methods, a sharp degradation may additionally indicate that the target domain has moved outside the uncertainty set implied by the sources (e.g., beyond the convex-hull condition). Fifth, our guarantees formalize robustness of reconstruction criteria, not invariance or stability: for example, a direction shared across domains need not be selected if it explains little variance in each domain. Investigating notions closer to invariance seems a promising route with potential connections to causality.

Acknowledgments and Disclosure of Funding

We thank Jacob Nelson for facilitating access to the FLUXNET data and preparing it for our use, and Maybritt Schillinger for many helpful discussions. We also thank Francesco Freni for helpful discussions on optimization and Linus Kühne for ideas related to Section 5.1.4. We have used LLMs for debugging code and improving language formulations.

References

- J. Ansel, E. Yang, H. He, N. Gimelshein, A. Jain, M. Voznesensky, B. Bao, P. Bell, D. Berard, E. Burovski, G. Chauhan, et al. PyTorch 2: Faster machine learning through dynamic python bytecode transformation and graph compilation. In *29th ACM International Conference on Architectural Support for Programming Languages and Operating Systems, Volume 2 (ASPLOS '24)*. ACM, 2024.

- P. Babu and P. Stoica. Fair principal component analysis (PCA): minorization-maximization algorithms for fair PCA, fair robust PCA and fair sparse PCA, 2023.
- D. Baldocchi. ‘Breathing’ of the terrestrial biosphere: lessons learned from a global network of carbon dioxide flux measurement systems. *Australian Journal of Botany*, 56(1):1–26, 2008.
- A. Ben-Tal, D. den Hertog, A. De Waegenaere, B. Melenberg, and G. Rennen. Robust solutions of optimization problems affected by uncertain probabilities. *Management Science*, 59(2):341–357, 2013.
- P. Bühlmann and N. Meinshausen. Maging: Maximin aggregation for inhomogeneous large-scale data. *Proceedings of the IEEE*, 104(1):126–135, 2016.
- E. Candès and B. Recht. Exact matrix completion via convex optimization. *Commun. ACM*, 55(6):111–119, 2012.
- E. J. Candès and Y. Plan. Matrix completion with noise. *Proceedings of the IEEE*, 98(6):925–936, 2010.
- R. D. Cook. Detection of influential observation in linear regression. *Technometrics*, 19(1):15–18, 1977.
- R. D. Cook and S. Weisberg. Assessment of influence. In *Residuals and Influence in Regression*, pages 135–137. Chapman and Hall, New York, 1982.
- J. C. Duchi and H. Namkoong. Variance-based regularization with convex objectives. *Journal of Machine Learning Research*, 20(68):1–55, 2019.
- B. N. Flury. Asymptotic theory for common principal component analysis. *The Annals of Statistics*, pages 418–430, 1986.
- B. N. Flury. Two generalizations of the common principal component model. *Biometrika*, 74(1):59–69, 1987.
- F. Freni, A. Fries, L. Kühne, M. Reichstein, and J. Peters. Maximum risk minimization with random forests, 2025.
- Z. Guo. Statistical inference for maximin effects: Identifying stable associations across multiple studies. *Journal of the American Statistical Association*, 119(547):1968–1984, 2024.
- K. R. Gurney, R. M. Law, A. S. Denning, P. J. Rayner, D. Baker, P. Bousquet, L. Bruhwiler, Y. Chen, P. Ciais, S. Fan, et al. Towards robust regional estimates of CO₂ sources and sinks using atmospheric transport models. *Nature*, 415(6872):626–630, 2002.
- K. R. Gurney, R. M. Law, A. S. Denning, P. J. Rayner, B. C. Pak, D. Baker, P. Bousquet, L. Bruhwiler, Y. Chen, P. Ciais, et al. Transcom 3 inversion intercomparison: model mean results for the estimation of seasonal carbon sources and sinks. *Global Biogeochemical Cycles*, 18(1), 2004.

- A. Hannachi, K. Finke, and N. Trendafilov. Common EOFs: a tool for multi-model comparison and evaluation. *Climate Dynamics*, 60(5):1689–1703, 2023.
- F. M. Harper and J. A. Konstan. The MovieLens datasets: History and context. *ACM Trans. Interact. Intell. Syst.*, 5(4), 2015.
- R. A. Horn and C. R. Johnson. Hermitian and symmetric matrices. In *Matrix Analysis*, pages 167–256. Cambridge University Press, Cambridge, 1985.
- W. Hu, G. Niu, I. Sato, and M. Sugiyama. Does distributionally robust supervised learning give robust classifiers? In *International Conference on Machine Learning (ICML)*, pages 2029–2037. PMLR, 2018.
- P. Jain and I. S. Dhillon. Provable inductive matrix completion, 2013.
- P. Jain, P. Netrapalli, and S. Sanghavi. Low-rank matrix completion using alternating minimization. In *Proceedings of the Forty-Fifth Annual ACM Symposium on Theory of Computing*, pages 665–674, 2013.
- I. T. Joliffe. Mathematical and statistical properties of population principal components. In *Principal Component Analysis*, pages 10–28. Springer New York, New York, NY, 2002.
- M. M. Kamani, F. Haddadpour, R. Forsati, and M. Mahdavi. Efficient fair principal component analysis. *Machine Learning*, pages 1–32, 2022.
- L. Kassab, E. George, D. Needell, H. Geng, N. J. Nia, and A. Li. Towards a fairer non-negative matrix factorization, 2024.
- Y. Koren, R. Bell, and C. Volinsky. Matrix factorization techniques for recommender systems. *Computer*, 42(8):30–37, 2009.
- S. Liu, Y. Ge, S. Xu, Y. Zhang, and A. Marian. Fairness-aware federated matrix factorization. In *Proceedings of the 16th ACM Conference on Recommender Systems, RecSys '22*, pages 168–178, New York, NY, USA, 2022. Association for Computing Machinery.
- M. W. Mahoney. Randomized algorithms for matrices and data. *Foundations and Trends® in Machine Learning*, 3(2):123–224, 2011.
- N. Meinshausen and P. Bühlmann. Maximin effects in inhomogeneous large-scale data. *The Annals of Statistics*, 43(4):1801–1830, 2015.
- M. Migliavacca, T. Musavi, M. D. Mahecha, J. A. Nelson, J. Knauer, D. D. Baldocchi, O. Perez-Priego, R. Christiansen, J. Peters, et al. The three major axes of terrestrial ecosystem function. *Nature*, 598(7881):468–472, 2021.
- G. Pastorello, C. Trotta, E. Canfora, H. Chu, D. Christianson, Y. Cheah, C. Poindexter, J. Chen, A. Elbashandy, M. Humphrey, et al. The FLUXNET2015 dataset and the ONEFlux processing pipeline for eddy covariance data. *Scientific data*, 7(1):225, 2020.
- P. Puchhammer, I. Wilms, and P. Filzmoser. Sparse outlier-robust PCA for multi-source data, 2024.

- S. Sagawa, P. W. Koh, T. B. Hashimoto, and P. Liang. Distributionally robust neural networks for group shifts: On the importance of regularization for worst-case generalization, 2020.
- S. Samadi, U. Tantipongpipat, J. H. Morgenstern, M. Singh, and S. Vempala. The price of fair PCA: One extra dimension. *Advances in Neural Information Processing Systems*, 31, 2018.
- A. Sinha, H. Namkoong, R. Volpi, and J. C. Duchi. Certifying some distributional robustness with principled adversarial training, 2017.
- U. Tantipongpipat, S. Samadi, M. Singh, J. H. Morgenstern, and S. Vempala. Multi-criteria dimensionality reduction with applications to fairness. *Advances in Neural Information Processing Systems*, 32, 2019.
- A. W. van der Vaart. M- and Z-estimators. In *Asymptotic Statistics*, Cambridge Series in Statistical and Probabilistic Mathematics, pages 41–84. Cambridge University Press, 1998.
- Z. Wang, M. Liu, J. Lei, F. Bach, and Z. Guo. StablePCA: Learning shared representations across multiple sources via minimax optimization, 2025.
- G. Zalcborg and A. Wiesel. Fair principal component analysis and filter design. *IEEE Transactions on Signal Processing*, 69:4835–4842, 2021.

Contents of the Appendix

| | | |
|----------|--|-----------|
| A | Additional details on wcPCA | 29 |
| B | Additional experimental details and results | 32 |
| C | Additional application details | 38 |
| D | Proofs | 40 |

Appendix A. Additional details on wcPCA

A.1 Sequential versus joint optimization for minPCA

This section provides a formal version of Proposition 4. In particular, we show that the sequential extension of PCA to the minPCA objective can fail to recover the solution of the corresponding joint optimization problem.

Proposition 14 *Consider Setting 1. Define $V_k^{seq-minPCA} := [v_1, \dots, v_k] \in \mathbb{R}^{p \times k}$ as k orthonormal vectors such that*

$$v_1 \in \arg \max_{v \in \mathbb{R}^p, \|v\|=1} \min_{e \in \mathcal{E}} \mathcal{L}_{\text{var}}(v; P_e)$$

$$v_j \in \arg \max_{\substack{v \in \mathbb{R}^p, \|v\|=1, \\ \forall i < j, v \perp v_i}} \min_{e \in \mathcal{E}} \mathcal{L}_{\text{var}}([v_1, \dots, v_{j-1}, v]; P_e) \quad \text{for } 2 \leq j \leq k.$$

Then, in general, $V_k^{seq-minPCA}$ does not solve minPCA.

Proposition 15 (Normalized case) *The statement of Proposition 14 holds for the normalized objective, that is, when \mathcal{L}_{var} is replaced by $\mathcal{L}_{\text{normVar}}$.*

Proof The same counter-example can be used to prove both statements; we present it in terms of minPCA. Consider three domains $\mathcal{E} = \{1, 2, 3\}$ with $p = 5$ and the following diagonal population covariances:

$$\Sigma_1 := \frac{1}{4} \text{diag}(2, 2, 0, 1, 1), \quad \Sigma_2 := \frac{1}{4} \text{diag}(2, 0, 2, 1, 1), \quad \Sigma_3 := \frac{1}{4} \text{diag}(0, 2, 2, 1, 1).$$

We find a rank-2 solution of the sequential procedure and then show that it is not optimal for the joint objective.

Step 1: We determine the first sequential component, i.e.,

$$v_1^* \in \arg \max_{v \in \mathbb{R}^5; \|v\|=1} \min_{e \in \mathcal{E}} v^\top \Sigma_e v.$$

Let $v_1^* = (a, b, c, d, f) \in \mathbb{R}^5$, $\|v_1^*\| = 1$. Then, $a^2 = b^2 = c^2$. We show this by contradiction. Since a, b , and c appear symmetrically in the objective, i.e., $\min_{e \in \mathcal{E}} (v_1^*)^\top \Sigma_e v_1^* = \frac{1}{2} \min(a^2 + b^2, b^2 + c^2, a^2 + c^2) + \frac{1}{4}(d^2 + f^2)$, we assume w.l.o.g. that $a^2 \leq b^2 \leq c^2$. Then, $\min_{e \in \mathcal{E}} (v_1^*)^\top \Sigma_e v_1^* = \frac{1}{2}(a^2 + b^2) + \frac{1}{4}(d^2 + f^2) =: m_1^*$. We consider the two cases

that lead to strict inequalities. First, if $a^2 < b^2$, let $\delta := \frac{1}{4}(b^2 - a^2) > 0$ and let $\tilde{v} := (\sqrt{a^2 + \delta}, \sqrt{b^2 - \delta/2}, \sqrt{c^2 - \delta/2}, d, f)$. Then, $\min_{e \in \mathcal{E}} \tilde{v}^\top \Sigma_e \tilde{v} = \frac{1}{2}(a^2 + b^2) + \frac{1}{4}(d^2 + f^2) + \frac{1}{4}\delta > m_1^*$. Second, if $a^2 = b^2$ and $b^2 < c^2$, let $\delta := \frac{1}{4}(c^2 - b^2)$ and let $\tilde{v} = (\sqrt{b^2 + \delta/2}, \sqrt{b^2 + \delta/2}, \sqrt{c^2 - \delta}, d, f)$. Then, $\min_{e \in \mathcal{E}} \tilde{v}^\top \Sigma_e \tilde{v} = a^2 + \frac{1}{4}(d^2 + f^2) + \frac{1}{2}\delta > m_1^*$. Hence, this proves that $a^2 = b^2 = c^2$. Then, $\|v_1^*\| = 1$ implies $3a^2 + d^2 + f^2 = 1$. Hence,

$$\min_{e \in \mathcal{E}} (v_1^*)^\top \Sigma_e v_1^* = 0.25 + 0.25a^2.$$

This is maximized for $a^2 = 1/3$, yielding $v_1^* := \frac{1}{\sqrt{3}}(1, 1, 1, 0, 0)$.

Step 2: We determine the second sequential component, i.e.,

$$v_2^* \in \arg \max_{\substack{v \in \mathbb{R}^5; \|v\|=1; \\ v \perp v_1^*}} \min_{e \in \mathcal{E}} \left\{ v^\top \Sigma_e v + (v_1^*)^\top \Sigma_e v_1^* \right\} = \arg \max_{\substack{v \in \mathbb{R}^5; \|v\|=1; \\ v \perp v_1^*}} \min_{e \in \mathcal{E}} v^\top \Sigma_e v + \frac{1}{3}.$$

Let $v_2^* = (a, b, c, d, f)$. $v_2^* \perp v_1^*$ implies $a = -(b + c)$ and $\|v_2^*\| = 1$ implies $d^2 + f^2 = 1 - a^2 - b^2 - c^2$. Simplifying gives

$$\min_{e \in \mathcal{E}} \left\{ (v_2^*)^\top \Sigma_e v_2^* + (v_1^*)^\top \Sigma_e v_1^* \right\} = \frac{1}{3} + \frac{1}{4} + \frac{1}{2} \min_{e \in \mathcal{E}} \{b^2 + bc, -bc, c^2 + bc\}.$$

For all $b, c \in \mathbb{R}$, $\min\{b^2 + bc, -bc, c^2 + bc\} \leq 0$ with equality if and only if $bc = 0$ or $b = -c$. Thus, the sequential solution has explained variance at most $\frac{1}{3} + \frac{1}{4} = \frac{7}{12}$.

Step 3: We show that the sequential solution is suboptimal for **minPCA**. Consider the rank-2 orthonormal matrix $\tilde{V} := [\tilde{v}_1, \tilde{v}_2]$ where $\tilde{v}_1 := \frac{1}{\sqrt{2}}(1, 1, 0, 0, 0)$ and $\tilde{v}_2 := \frac{1}{\sqrt{2}}(0, 0, 1, 1, 0)$. For each domain, the total variance equals $\frac{5}{8}$, which is strictly larger than $\frac{7}{12}$. Thus, the sequential solution does not solve **minPCA**. \blacksquare

A.2 Ordering the basis of norm-maxRCS

Sequential constructions are, in general, not optimal for the joint worst-case objective (see Proposition 14). Nevertheless, in some applications an ordered basis is required. We therefore describe a post-hoc procedure that imposes an ordering within the optimal worst-case subspace. We present the construction for **norm-minPCA**; the same idea can be applied to the other objectives.

Consider Setting 1 and let $V_k^* \in \mathbb{R}^{p \times k}$ solve **norm-minPCA**. Starting with the full subspace $S_1 := \text{span}(V_k^*)$, we iteratively identify and remove the direction whose removal maximizes the worst-case explained variance of the remaining subspace. For $i \in \{1, \dots, k-1\}$, let

$$v_i \in \arg \max_{\substack{v \in \text{span}(V_i^*); \\ \|v\|=1}} \min_{e \in \mathcal{E}} \frac{1}{\text{Tr}(\Sigma_e)} \text{Tr} \left(U_{S_i \cap v^\perp}^\top \Sigma_e U_{S_i \cap v^\perp} \right),$$

where $S_{i+1} := \text{span}(V_k^*) \cap \text{span}(\{v_1, \dots, v_i\})^\perp$ and for any subspace $S \subset \mathbb{R}^p$, U_S denotes an orthonormal basis of S . Reversing the resulting sequence (v_1, \dots, v_{k-1}) and appending the final remaining direction yields (v'_1, \dots, v'_k) such that, for any $j \leq k$, the span of (v'_1, \dots, v'_j) maximizes worst-case explained variance among all j -dimensional subspaces contained in $\text{span}(V_k^*)$.

A.3 Comparison to Group DRO

Group DRO (Sagawa et al., 2020; Hu et al., 2018) is a widely studied framework for robustness to distributional shifts across a finite set of domains. Our guarantees share a similar structure but apply to a broader class of distributions and rely on weaker assumptions.

Remark 16 *In Group DRO, the goal is to minimize the worst-case loss over a finite set of distributions $\{P_e\}_{e \in \mathcal{E}}$. Losses of the form $\mathcal{L}(V; P) = \mathbb{E}_{\mathbf{x} \sim P}[\ell(V; \mathbf{x})]$ are linear with respect to convex combinations of distributions. The worst-case loss over all mixtures of the source distributions (i.e., the convex hull of the source distributions) is thus attained at one of the source distributions, that is,*

$$\max_{e \in \mathcal{E}} \mathcal{L}(V; P_e) = \sup_{P \in \mathcal{Q}} \mathcal{L}(V; P) \quad \text{where} \quad \mathcal{Q} := \text{conv}(P_1, \dots, P_E). \quad (9)$$

Our results for maxRCS, and minPCA apply in this setting and are strictly stronger, establishing worst-case optimality over a strictly larger uncertainty set \mathcal{P} (based on covariance matrices rather than distributions, see (4)). even a weaker form of the result does not follow directly from Group DRO. For norm-maxRCS, norm-minPCA, and norm-maxRegret the loss is a ratio of expectations and thus not linear with respect to convex combinations of distributions. In this case, the standard Group DRO guarantees over the mixture of source distributions no longer hold, and our guarantees instead apply to an uncertainty set defined via constraints on the normalized covariance matrices.

A.4 Empirical objectives and finite-sample guarantees

This appendix collects the finite-sample counterparts of the worst-case objectives introduced in the main text that are not presented in Section 3.2. It also states the finite-sample optimality guarantees of the unnormalized objectives, which mirrors the population results (Theorem 6) with population covariances replaced by empirical covariances. Consider Setting 2. For $\hat{V} \in \mathcal{O}_{p \times k}$, we say

$$\hat{V} \text{ solves rank-}k \text{ empirical norm-minPCA if } \hat{V} \in \arg \max_{V \in \mathcal{O}_{p \times k}} \max_{e \in \mathcal{E}} \left\{ \frac{\text{Tr}(V^\top \hat{\Sigma}_e V)}{\text{Tr}(\hat{\Sigma}_e)} \right\},$$

$$\hat{V} \text{ solves rank-}k \text{ empirical norm-maxRCS if } \hat{V} \in \arg \min_{V \in \mathcal{O}_{p \times k}} \max_{e \in \mathcal{E}} \left\{ \frac{\|X_e - X_e V V^\top\|_F^2}{\|X_e\|_F^2} \right\},$$

\hat{V} solves rank- k empirical maxRegret if

$$\hat{V} \in \arg \min_{V \in \mathcal{O}_{p \times k}} \max_{e \in \mathcal{E}} \left\{ \|X_e - X_e V V^\top\|_F^2 - \left(\min_{W \in \mathcal{O}_{p \times k}} \|X_e - X_e W W^\top\|_F^2 \right) \right\},$$

and \hat{V} solves rank- k empirical norm-maxRegret if

$$\hat{V} \in \arg \min_{V \in \mathcal{O}_{p \times k}} \max_{e \in \mathcal{E}} \left\{ \frac{\|X_e - X_e V V^\top\|_F^2}{\|X_e\|_F^2} - \left(\min_{W \in \mathcal{O}_{p \times k}} \frac{\|X_e - X_e W W^\top\|_F^2}{\|X_e\|_F^2} \right) \right\}.$$

Proposition 17 (Empirical robustness of wcPCA) *Consider Setting 2 and let $\hat{\mathcal{C}} := \text{conv}(\{\hat{\Sigma}_e\}_{e \in \mathcal{E}})$ be the convex hull of the empirical source covariances. Let $\hat{V}_k \in \mathcal{O}_{p \times k}$ solve empirical rank- k **maxRCS**, **minPCA**, or **maxRegret**. Let \mathcal{L} denote the corresponding loss function, i.e., $\mathcal{L} = \mathcal{L}_{\text{RCS}}$ for **maxRCS**, $\mathcal{L} = -\mathcal{L}_{\text{var}}$ for **minPCA**, and $\mathcal{L} = \mathcal{L}_{\text{reg}}$ for **maxRegret**. Then, the following statements hold.*

i) *For all $V_k \in \mathcal{O}_{p \times k}$, the worst-case loss over $\hat{\mathcal{C}}$ equals the worst-case loss over the source domains, i.e.,*

$$\sup_{\Sigma \in \hat{\mathcal{C}}} \mathcal{L}(V_k; \Sigma) = \max_{e \in \mathcal{E}} \mathcal{L}(V_k; \hat{\Sigma}_e).$$

ii) *Consequently, the ordering induced by the worst-case loss over the source domains is preserved over $\hat{\mathcal{C}}$: for all $V_k, W_k \in \mathcal{O}_{p \times k}$, if $\max_{e \in \mathcal{E}} \mathcal{L}(V_k; \hat{\Sigma}_e) < \max_{e \in \mathcal{E}} \mathcal{L}(W_k; \hat{\Sigma}_e)$, then $\sup_{\Sigma \in \hat{\mathcal{C}}} \mathcal{L}(V_k; \Sigma) < \sup_{\Sigma \in \hat{\mathcal{C}}} \mathcal{L}(W_k; \Sigma)$.*

iii) *Hence, \hat{V}_k is worst-case optimal over $\hat{\mathcal{C}}$, i.e., $\hat{V}_k \in \arg \min_{V \in \mathcal{O}_{p \times k}} \sup_{\Sigma \in \hat{\mathcal{C}}} \mathcal{L}(V; \Sigma)$.*

iv) *Statement iii) does not generally hold for the solutions to empirical **poolPCA** and **sepPCA**.*

Appendix B. Additional experimental details and results

B.1 Data generating process for source and target covariances

In each experiment, we consider E source domains, obtained by sampling E population covariances matrices $(\Sigma_1, \dots, \Sigma_E)$ in $\mathbb{R}^{p \times p}$ of rank 10 from a measure $\mathbb{Q}_{\alpha, \beta}$ that depends on parameters α, β (explained below). Unless otherwise specified, $E = 5$ and $p = 20$. Under the measures $\mathbb{Q}_{\alpha, \beta}$, the sampled covariances consist of a rank-5 shared component and a rank-5 domain-specific component, and each of them is trace-normalized. For the simulations in Section 5.1.1–5.1.3 and Appendix B.2, the domain-specific components have an equal set of eigenvalues across domains, and for Section 5.1.4, these sets of eigenvalues vary across domains. We now describe the generation of the source covariances in more detail.

Source covariances. To sample E source covariances, denoted as $(\Sigma_1, \dots, \Sigma_E) \sim \mathbb{Q}_{\alpha, \beta}$, we proceed as follows.

1. Sample the eigenvalues and eigenvectors of the shared component as $\lambda_1, \dots, \lambda_5 \stackrel{\text{iid}}{\sim} U([0.1, 1])$ and $Q \sim \mathbb{P}_{\mathbb{O}}$, where $\mathbb{P}_{\mathbb{O}}$ denotes the Haar distribution over orthonormal matrices $Q \in \mathbb{R}^{p \times p}$ with $Q^\top Q = QQ^\top = I_p$. Let $V \in \mathbb{R}^{p \times 5}$ denote the first five columns of Q , forming an orthonormal basis of the shared rank-5 subspace, and let $\boldsymbol{\lambda} := (\lambda_1, \dots, \lambda_5) \in \mathbb{R}^5$.
2. Sample the eigenvalues of the domain-specific component as $\gamma_1, \dots, \gamma_5 \stackrel{\text{iid}}{\sim} U([\alpha, \beta])$ (unless otherwise specified, $\alpha = 0.1$ and $\beta = 1$). Let $\boldsymbol{\gamma} := (\gamma_1, \dots, \gamma_5) \in \mathbb{R}^5$ (we use the same $\boldsymbol{\gamma}$ for all source domains).
3. Sample the (domain-specific) eigenvectors of the domain-specific component as follows. For $1 \leq e \leq E$, sample a Gaussian matrix $G_e \in \mathbb{R}^{p \times 5}$ with i.i.d. standard normal

entries. Let $P_{\perp} := I - VV^T$ be the projector onto the orthogonal complement of $\text{span}(V)$. We define $V_e \in \mathbb{R}^{p \times 5}$ as the Q factor in the QR decomposition of $P_{\perp}G_e$. Then the columns of V_e form an orthonormal basis of a rank-5 subspace orthogonal to V .

4. For all $1 \leq e \leq E$, define

$$\Sigma_e := \frac{1}{\sum_{i=1}^5 (\lambda_i + \gamma_i)} \left(V \text{diag}(\boldsymbol{\lambda}) V^T + V_e \text{diag}(\boldsymbol{\gamma}) V_e^T \right).$$

Modifications for Section 5.1.4. In Section 5.1.4, we modify the procedure as follows. In step 2, instead of sampling shared domain-specific eigenvalues, we sample different eigenvalues for each domain. That is, for all domains $1 \leq e \leq E$, we sample $\gamma_1^e, \dots, \gamma_5^e \stackrel{\text{iid}}{\sim} U([\alpha, \beta])$ and let $\boldsymbol{\gamma}_e := (\gamma_1^e, \dots, \gamma_5^e) \in \mathbb{R}^5$. In step 4, we then replace the eigenvectors with the domain specific ones, that is, for all $1 \leq e \leq E$, for $1 \leq i \leq 5$, we replace γ_i with γ_i^e and we replace $\boldsymbol{\gamma}$ with $\boldsymbol{\gamma}_e$.

Target covariances. The set of target covariances, $\mathcal{C}_{\text{target}}^t$, consists of t covariances sampled i.i.d. from the convex hull of the source covariances, $\mathcal{C} := \text{conv}(\{\Sigma_e\}_{e=1}^E)$. Each target covariance Σ is obtained by sampling w uniformly from the E -dimensional simplex and setting $\Sigma = \sum_{e=1}^E w_e \Sigma_e$. The superscript t is omitted when the number of target covariances is clear from context.

B.2 Optimization algorithms

B.2.1 wcPCA

The optimization problems of the wcPCA variants are non-convex due to the orthogonality constraint set $\mathcal{O}_{p \times k}$. In principle, any optimization scheme designed for orthogonality constraints may be employed. Several relaxations have been proposed for some of the variants. Tantipongpipat et al. (2019) (FairPCA) provides a semidefinite programming (SDP) relaxation and multiplicative weights (MW) algorithm for the `minPCA` and `maxRegret` objectives. Wang et al. (2025) (StablePCA) provide an optimization scheme for `minPCA`, `maxRCS`, and `maxRegret` with convergence guarantees. Neither of them consider the other objectives. Other approaches, such as extra-gradient methods for saddle-point problems, may also apply in this setting but have not yet been explored for these objectives.

Our focus in this paper lies on the generalization guarantees rather than the optimization. For the implementation, we therefore employ a straightforward projected gradient descent (PGD) scheme implemented in PyTorch (Ansel et al., 2024), with updates computed via the Adam optimizer. Because the objectives involve pointwise maxima or minima, gradients are propagated only through the active component at each step. Concretely, with current estimate V_t , one iteration update is

$$\begin{aligned} \nabla \mathcal{L}(V_t) &\leftarrow \text{autograd}(\mathcal{L}, V), \\ V' &\leftarrow \text{AdamStep}(V_t, \nabla \mathcal{L}(V_t)), \\ V_{t+1} &\leftarrow \Pi_{\mathcal{O}_{p \times k}}(V'), \end{aligned}$$

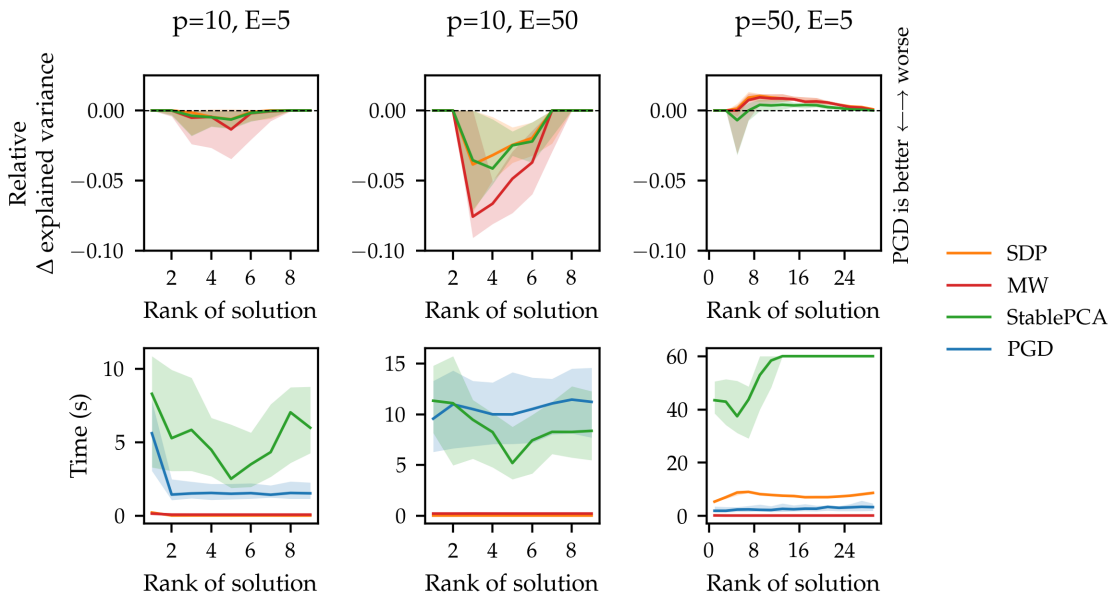


Figure B.i: Comparison of projected gradient descent (PGD; used in our experiments) with the optimization schemes of Wang et al. (2025) (StablePCA) and Tantipongpipat et al. (2019) (MW and SDP) for solving minPCA. Results are shown for $(p, E) \in \{(10, 5), (10, 50), (50, 5)\}$ where p is the number of features and E is the number of domains. *Top row*: median difference in minimum explained variance relative to that of PGD (negative values indicate that PGD explains more variance in the worst case) as a function of the number of components k . *Bottom row*: runtime in seconds for each algorithm. Shaded regions represent the 25%-75% quantiles. PGD attains similar objective values to both baselines, with acceptable runtime.

where $\Pi_{\mathcal{O}_{p \times k}}$ denotes projection onto $\mathcal{O}_{p \times k}$, implemented via an SVD-based orthogonalization. To mitigate poor local minima, we run five random restarts and retain the best solution.

To assess the effectiveness of our implementation, we compare the proposed PGD scheme with StablePCA and FairPCA. We consider three configurations for the number of features p and domains E : $(p, E) \in \{(10, 5), (10, 50), (50, 5)\}$, corresponding, respectively, to few features–few domains, few features–many domains, and many features–few domains. For each configuration, we repeat the following steps 25 times. We generate domain-specific covariance matrices as described in Appendix B.1. For $k = 1, \dots, \min(p - 1, 30)$, we solve the rank- k population minPCA problem using our PGD implementation, StablePCA (Wang et al., 2025) and the SDP and MW variants of Tantipongpipat et al. (2019). When the solution matrix is not rank- k in the output of the FairPCA optimization, we consider only the top k eigenvectors.

Figure B.i reports the median value of $(\text{minvar}_{\text{other}} - \text{minvar}_{\text{PGD}}) / |\text{minvar}_{\text{PGD}}|$ where $\text{minvar}_{\text{other}}$ and $\text{minvar}_{\text{PGD}}$ are, respectively, the minimum explained variance of the other optimization scheme and of PGD and the median running time. Across all configurations,

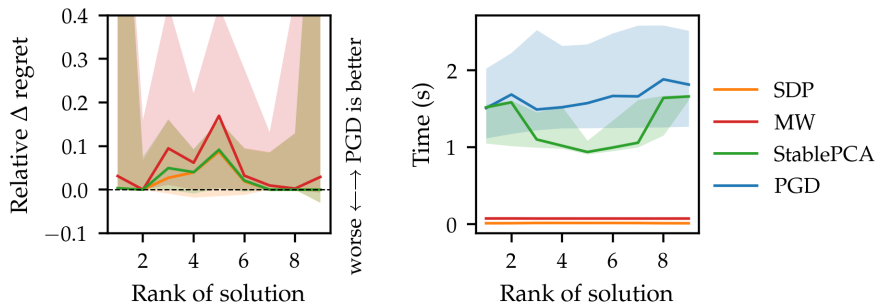


Figure B.ii: Comparison of PGD, StablePCA, MW, and SDP for solving $\max\text{Regret}$ for $(p, E) = (10, 5)$. PGD achieves comparable (or better) maximum regret values (positive values indicate that PGD performs better, i.e., has a lower worst-case regret).

the objective values obtained by PGD closely match those by StablePCA, SDP, and MW and for smaller problems, PGD explains more variance. For smaller problems, the SDP and MW optimization schemes are faster, whereas for higher-dimensional settings only MW is faster than PGD. As computational cost is not a limiting factor for our analysis, we use the PGD implementation throughout the paper. For completeness, we also consider solutions to population $\max\text{Regret}$ for $(p, E) = (10, 5)$ (shown in Figure B.ii), where PGD attains objective values on par with the other optimization schemes with runtimes that are acceptable for the purpose of our paper. Here, the other optimization schemes occasionally returns solutions with considerably worse (i.e., higher) objective value.

B.2.2 MATRIX COMPLETION

The matrix completion objectives poolMC and maxMC are non-convex in $(L_e, R)_{e \in \mathcal{E}}$, due to the bilinear term $L_e R^\top$ (see (6)). We therefore employ a standard alternating-minimization scheme, iteratively updating R given $(L_e)_{e \in \mathcal{E}}$ and then $(L_e)_{e \in \mathcal{E}}$ given R . This scheme is similar to what Kassab et al. (2024) propose for a regret-based variant of fair matrix completion and to what is commonly done in the pooled case (e.g., Jain et al., 2013) – even though in the pooled case, there is only a single left factor. Our implementation is adapted from Aaron Berk’s implementation of alternating minimization for single-domain matrix completion⁸. More precisely, given current left factors $(L_e)_{e \in \mathcal{E}}$, we update the shared right factor R by solving a convex optimization problem. For maxMC , this step minimizes the maximum (across domains) of the normalized reconstruction error over the observed entries; for poolMC , it minimizes the pooled reconstruction error across all observed entries. Both problems are formulated and solved as second-order cone programs in `cvxpy`. Given R , the left-factor updates decouple across domains and rows. Thus, for each domain e and row i , we estimate $\ell_{e,i}$ via the inductive least-squares reconstruction rule of Section 4.1, restricted to the entries observed in that row. The alternating updates are run for at most 100 iterations and terminated early when the improvement in the objective falls below 10^{-4} . Initialization of $\{L_e\}$ is done using an SVD-based heuristic obtained by filling a sparse matrix with the observed entries.

8. <https://github.com/asberk/matrix-completion-whirlwind>

B.3 Evaluation metrics

This appendix defines the evaluation metrics used in Sections 5.1.2, 5.1.3, and 5.2. Let $\mathcal{E} := \{1, \dots, 5\}$, $\mathcal{C}_{\text{source}} := \{\Sigma_1, \dots, \Sigma_5\}$ denote the set of source covariances and $\mathcal{C} := \text{conv}(\mathcal{C}_{\text{source}})$ denote their convex hull. Recall that for a covariance matrix Σ , for all $V \in \mathcal{O}_{p \times k}$ the reconstruction loss is $\mathcal{L}_{\text{RCS}}(V; \Sigma) = \text{Tr}(\Sigma) - \text{Tr}(V^\top \Sigma V)$.

Average and worst-case performance (see Section 5.1.2). Let $\bar{\Sigma} := \frac{1}{|\mathcal{E}|} \sum_{e \in \mathcal{E}} \Sigma_e$ be the average covariance and let V^{maxRCS} and V^{pool} solve **maxRCS** and **poolPCA**. The difference in average reconstruction error (over the source domains) relative to the average performance of **poolPCA** is

$$\Delta \text{ average} := \frac{\mathcal{L}_{\text{RCS}}(V^{\text{maxRCS}}; \bar{\Sigma}) - \mathcal{L}_{\text{RCS}}(V^{\text{pool}}; \bar{\Sigma})}{\mathcal{L}_{\text{RCS}}(V^{\text{pool}}; \bar{\Sigma})}. \quad (10)$$

The difference in worst-case reconstruction error (over the convex hull of the source covariances), relative to the average performance of **poolPCA** is

$$\Delta \text{ worst-case} := \frac{\sup_{\Sigma \in \mathcal{C}} \mathcal{L}_{\text{RCS}}(V^{\text{maxRCS}}; \Sigma) - \sup_{\Sigma \in \mathcal{C}} \mathcal{L}_{\text{RCS}}(V^{\text{pool}}; \Sigma)}{\mathcal{L}_{\text{RCS}}(V^{\text{pool}}; \bar{\Sigma})}. \quad (11)$$

Since \mathcal{L}_{RCS} is linear in Σ , the supremum over \mathcal{C} is attained at its extreme points; in practice, it is computed as a maximum over the source covariances. The quantities (10) and (11) correspond to the values plotted in Figure 4.

Convergence and finite-sample robustness (see Section 5.1.3). To assess convergence of the empirical estimator \hat{V}^{maxRCS} to the population solution V^{maxRCS} , we compute the difference in worst-case population reconstruction error (evaluated over the convex hull $\text{conv}(\mathcal{C}_{\text{source}})$):

$$\sup_{\Sigma \in \mathcal{C}} \mathcal{L}_{\text{RCS}}(\hat{V}^{\text{maxRCS}}; \Sigma) - \sup_{\Sigma \in \mathcal{C}} \mathcal{L}_{\text{RCS}}(V^{\text{maxRCS}}; \Sigma). \quad (12)$$

This metric corresponds to the quantity plotted in Figure 5 (left). To compare finite-sample robustness of empirical **maxRCS** and empirical **poolPCA**, we additionally report

$$\sup_{\Sigma \in \mathcal{C}} \mathcal{L}_{\text{RCS}}(\hat{V}^{\text{maxRCS}}; \Sigma) - \sup_{\Sigma \in \mathcal{C}} \mathcal{L}_{\text{RCS}}(\hat{V}^{\text{pool}}; \Sigma). \quad (13)$$

This metric corresponds to Figure 5 (right). Negative values indicate that the empirical **maxRCS** estimator achieves lower worst-case population loss than pooled PCA. Again, in practice, the supremum is computed as a maximum over the source covariances.

Matrix completion (see Section 5.2). For the matrix completion experiments, for all $e \in \mathcal{E}$, let $X_e \in \mathbb{R}^{n_{\text{test}} \times p}$ denote the matrix of test observations from domain e , and for all $R \in \mathcal{O}_{p \times k}$, let $\hat{X}_e(R)$ denote their reconstructions obtained using the inductive least-squares rule of Section 4.1. For each domain $e \in \mathcal{E}$, we define the per-entry mean squared reconstruction error as

$$\mathcal{L}_e(R) := \frac{1}{n_{\text{test}} p} \|X_e - \hat{X}_e(R)\|_F^2.$$

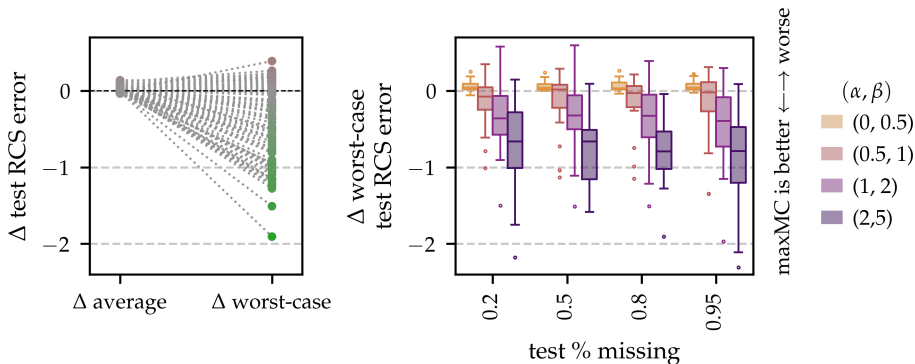


Figure B.iii: *Worst-case inductive matrix completion with fully observed source domains; regime (i)*. *Left*: Difference in average and worst-case test reconstruction error between **maxMC** and **poolMC**. In line with Theorem 13 (which covers the population case and allows for some ϵ deviation), **maxMC** generally improves worst-case performance; in terms of average error, it incurs only minor changes. *Right*: Worst-case difference as the proportion of missing target entries varies, for different heterogeneity levels (α, β) . **maxMC** achieves lower median worst-case error than **poolMC**, with larger gains under stronger domain heterogeneity.

Let R^{maxMC} and R^{poolMC} solve **maxMC** and **poolMC**, respectively. We consider the difference in average and worst-case performance, that is,

$$\begin{aligned} \Delta \text{ average} &:= \frac{1}{|\mathcal{E}|} \sum_{e \in \mathcal{E}} (\mathcal{L}_e(R^{\text{maxMC}}) - \mathcal{L}_e(R^{\text{poolMC}})), \\ \Delta \text{ worst-case} &:= \max_{e \in \mathcal{E}} \mathcal{L}_e(R^{\text{maxMC}}) - \max_{e \in \mathcal{E}} \mathcal{L}_e(R^{\text{poolMC}}). \end{aligned}$$

Negative values indicate that **maxMC** achieves lower error than **poolMC**. In Figure 7, we report $10^4 \cdot \Delta \text{ average}$ and $10^4 \cdot \Delta \text{ worst-case}$.

B.4 Inductive matrix completion with fully observed sources

We consider the regime in which the source domains are fully observed, corresponding to the setting of Theorem 13, while target domains remain partially observed. In this case, **maxMC** reduces to **maxRCS** on the source data. Consistent with the theory, **maxMC** typically achieves lower worst-case target reconstruction error than **poolMC** (Figure B.iii). For low domain heterogeneity, however, the empirical advantage is occasionally negligible or slightly reversed. This can be attributed to (i) the fact that Theorem 13 provides an approximate worst-case guarantee rather than a strict improvement over pooling, and (ii) finite-sample variability and non-optimality when solving the non-convex optimization procedure, for which improved algorithms may yield tighter empirical performance. Overall, the results mirror those in Section 5.2: the worst-case advantage of **maxMC** is most pronounced under stronger domain heterogeneity and persists across varying levels of missingness.

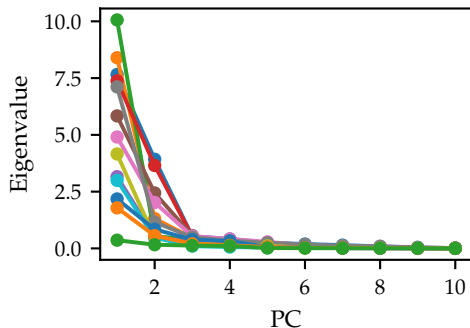


Figure C.i: Scree plots for each TransCom region (shown in different colours). In Section 6.1, we use rank-2 approximations.

Appendix C. Additional application details

C.1 Details on the FLUXNET application (Section 6.1)

Data preprocessing. We use quality-controlled FLUXNET data (Pastorello et al., 2020), aggregated to daily means. Let us denote the thirteen TransCom regions as \mathcal{E} . For each TransCom region $e \in \mathcal{E}$ with data matrix $X_e^{\text{raw}} \in \mathbb{R}^{n_e \times p}$, we first remove the domain mean and denote the centered matrix by \tilde{X}_e . We then stack the centered data $\tilde{X} := [\tilde{X}_1; \dots; \tilde{X}_E]$ and compute pooled columnwise standard deviations on \tilde{X} . Using these, we standardise \tilde{X} to obtain X_{pool} , and for each $e \in \mathcal{E}$, we define X_e as the corresponding block of rows of X_{pool} belonging to domain e . For all $e \in \mathcal{E}$, the empirical covariances are $\hat{\Sigma}_e = \frac{1}{n_e} X_e^\top X_e$, and the pooled covariance equals the weighted sum $\hat{\Sigma}_{\text{pooled}} = \frac{1}{n} X_{\text{pool}}^\top X_{\text{pool}} = \sum_e w_e \hat{\Sigma}_e$ where $n = \sum_j n_j$ and $w_e = n_e/n$. The average covariance is given by $\frac{1}{|\mathcal{E}|} \sum_{e \in \mathcal{E}} \hat{\Sigma}_e$. Intuitively, this preprocessing removes between-region mean shifts and focuses the analysis on differences in covariance structure across regions.

Choosing the number of principal components. Based on scree plots of the source regions (Figure C.i), the explained variance levels off after the second component. We thus use rank-2 approximations in Section 6.1.

Random splits of source and target regions. For 20 repetitions, the TransCom regions are randomly partitioned into five source regions and eight target regions. Figure C.ii reports the relative difference in worst-case proportion of explained variance between poolPCA and the competing methods (maxRegret, norm-maxRegret, norm-maxRCS, avgcovPCA) over the repetitions — shown across ranks and on the source and target domains.

C.2 Details on the reanalysis of Migliavacca et al. (2021) (Section 6.2)

Data description and preprocessing. We use the site-level ecosystem function dataset constructed by Migliavacca et al. (2021), based on FLUXNET observations (Baldocchi, 2008; Pastorello et al., 2020). Each site contributes a single vector of aggregated functional properties (described in Table 2). We define continents as domains. Preprocessing follows

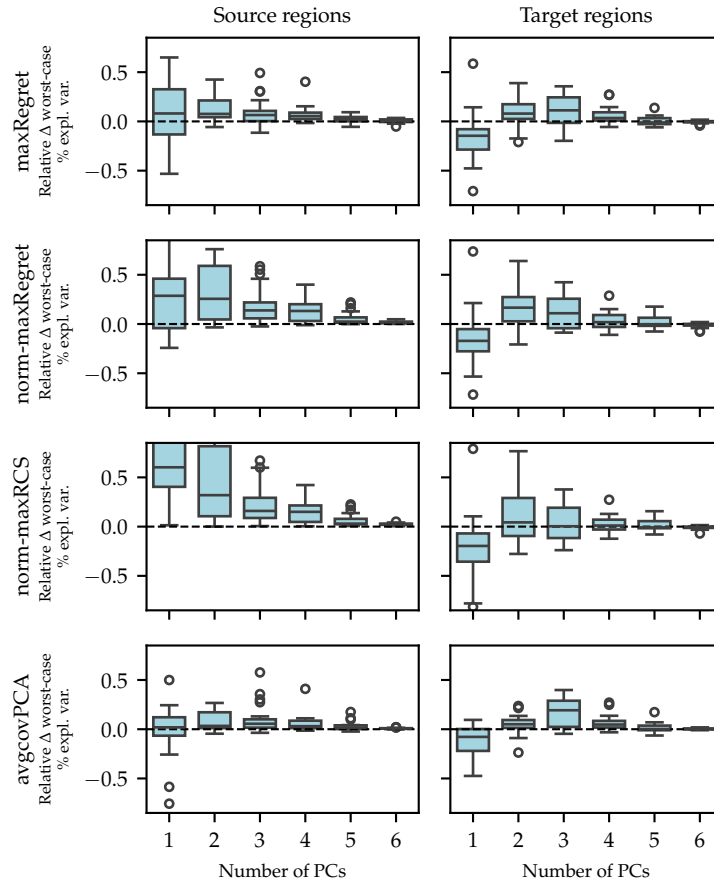


Figure C.ii: Relative difference in worst-case proportion of explained variance between `poolPCA` and, from top to bottom, `maxRegret`, `norm-maxRegret`, `norm-maxRCS`, and `avgcovPCA`. Positive values indicate improved worst-case performance relative to `poolPCA`. Results are shown for 20 random region splits, evaluated on the source and target regions across varying numbers of principal components. Apart from the rank-one case, the worst-case objectives exhibit improved robustness or similar behavior to `poolPCA`.

the procedure described in Appendix C.1, with continents replacing the TransCom regions.

Additional methods. As an additional baseline, we solve PCA on the unweighted average of the domain covariance matrices ($\frac{1}{|\mathcal{E}|} \sum_{e \in \mathcal{E}} \hat{\Sigma}_e$), denoted `avgcovPCA`. This estimator removes the implicit weighting of domains by sample size present in `poolPCA`. In addition, we fit `maxRegret`. Figure C.iii reports the corresponding performance and shows that `maxRegret` performs almost identically to `norm-maxRegret`. Using the average covariance instead of `poolPCA` substantially improves worst-case performance, but it remains slightly inferior to `norm-maxRCS` both in average explained variance and in the worst-performing continent. However, to the best of our knowledge, `avgcovPCA` does not come with any extrapolation guarantee.

Table 2: Ecosystem functional properties used in the reanalysis of Migliavacca et al. (2021).

| Variable | Description |
|--------------------|--|
| GPP_{sat} | Maximum gross CO ₂ uptake at light saturation |
| NEP_{max} | Maximum net ecosystem productivity |
| ET_{max} | Maximum evapotranspiration |
| EF | Evaporative fraction |
| EF_{ampl} | EF amplitude |
| GS_{max} | Maximum dry canopy surface conductance |
| Rb | Mean basal ecosystem respiration |
| RB_{max} | Maximum basal ecosystem respiration |
| aCUE | Apparent carbon-use efficiency (fraction of assimilated carbon retained) |
| uWUE | Underlying water-use efficiency |
| WUE_t | Transpiration-based water-use efficiency |
| G1 | Ecosystem-scale stomatal slope parameter |

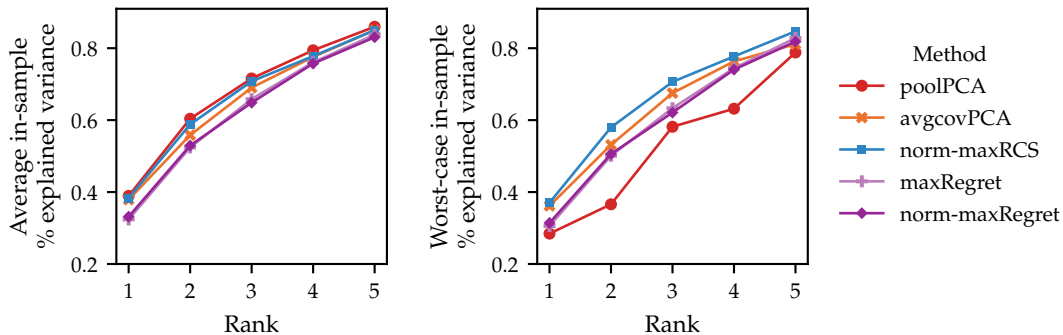


Figure C.iii: Comparison of dimensionality reduction methods on the ecosystem function dataset. *Left*: Proportion of variance explained on the pooled dataset. *Right*: Worst-case proportion of variance explained across continents. Methods that account for domain heterogeneity outperform poolPCA in the worst-case continent, with norm-maxRCS most closely matching pooled average performance.

Appendix D. Proofs

D.1 Additional results

There are several variations of the following statement that are known, both for single-case deletion, that is, Cook’s formula (Cook, 1977), and for subset removal (e.g., Section 3.6 in Cook and Weisberg, 1982). Bounding this perturbation via μ -incoherence (Candès and Recht, 2012) is a standard technique in randomized linear algebra (Mahoney, 2011). We add the proof for completeness.

Proposition 18 (Stability of OLS under subset removal) *Let $X \in \mathbb{R}^{n \times p}$ be a deterministic design matrix satisfying the orthogonality condition $X^\top X = I_p$ and the μ -*

incoherence condition:

$$\|x^{(i)}\|_2 \leq \mu \sqrt{\frac{p}{n}}, \quad \forall i \in \{1, \dots, n\}, \quad (14)$$

where $x^{(i)}$ is the i -th row of X . Let $y \in \mathbb{R}^n$ be a response vector. Let β^* be the OLS estimator on the full dataset. Consider any subset $S \subseteq \{1, \dots, n\}$, define $s := |S|$, and let X_{-S} (resp. y_{-S}) denote the submatrix (resp. subvector) of X (resp. y) consisting of the rows (resp. entries) indexed by $[n] \setminus S$. Let β_{-S} be the OLS estimator on the dataset without the entries in S , that is, $\beta_{-S} \in \arg \min_{b \in \mathbb{R}^p} \|y_{-S} - X_{-S}b\|_2^2$. For all $\epsilon \in (0, 1)$, if the subset size s satisfies

$$s \leq \frac{n\epsilon}{p\mu^2(2\epsilon + 1)} \quad (15)$$

then the relative increase in squared error is bounded by ϵ , that is,

$$\|y - X\beta_{-S}\|_2^2 \leq (1 + \epsilon)\|y - X\beta^*\|_2^2.$$

Proof First, we show that β_{-S} is unique (step 1), then we bound the difference between the reconstruction error of β^* and β_{-S} (step 2).

Step 1: We show that $X_{-S}^\top X_{-S}$ is invertible, which implies that β_{-S} is uniquely defined. Let X_S (resp. y_S) denote the sub-matrix (resp. sub-vector) of X (resp. y) consisting of the rows (resp. entries) indexed by S . The spectral norm (denoted by $\|\cdot\|_{op}$) of X_S is bounded as follows

$$\|X_S\|_{op}^2 \leq \text{Tr}(X_S^\top X_S) = \sum_{i \in S} \|x^{(i)}\|_2^2 \leq s \cdot \frac{\mu^2 p}{n} < 1, \quad (16)$$

where the second inequality follows from the incoherence condition (14) and the third inequality follows from the subset size assumption (15). Hence, the maximum eigenvalue $\lambda_{\max}(X_S^\top X_S) < 1$ and thus $I_p - X_S^\top X_S = X_{-S}^\top X_{-S}$ is invertible and β_{-S} is unique and given by

$$\beta_{-S} = (X_{-S}^\top X_{-S})^{-1} X_{-S}^\top y_{-S} = (I - X_S^\top X_S)^{-1} (X^\top y - X_S^\top y_S). \quad (17)$$

Step 2: We now bound the reconstruction error using β_{-S} as

$$\begin{aligned} \|y - X\beta_{-S}\|_2^2 &= \|y - X\beta^* + X\beta^* - X\beta_{-S}\|_2^2 \\ &= \|y - X\beta^*\|_2^2 + \|X\beta^* - X\beta_{-S}\|_2^2 \\ &= \|y - X\beta^*\|_2^2 + \|\beta^* - \beta_{-S}\|_2^2, \end{aligned}$$

where the first equality follows as $X^\top(y - X\beta^*) = 0$ and the last equality follows as X is orthogonal. It thus suffices to bound $\|\beta^* - \beta_{-S}\|_2^2$ which we do using (17) as follows,

$$\begin{aligned} \|\beta^* - \beta_{-S}\|_2^2 &= \|\beta^* - (I - X_S^\top X_S)^{-1} (X^\top y - X_S^\top y_S)\|_2^2 \\ &= \|(I - X_S^\top X_S)^{-1} (I - X_S^\top X_S) \beta^* - (I - X_S^\top X_S)^{-1} (\beta^* - X_S^\top y_S)\|_2^2 \\ &= \|(I - X_S^\top X_S)^{-1} X_S^\top (y_S - X_S \beta^*)\|_2^2 \\ &\leq \|(I - X_S^\top X_S)^{-1}\|_{op}^2 \|X_S^\top\|_{op}^2 \|y_S - X_S \beta^*\|_2^2 \\ &\leq \|(I - X_S^\top X_S)^{-1}\|_{op}^2 \|X_S^\top\|_{op}^2 \|y - X\beta^*\|_2^2. \end{aligned}$$

In addition, $\|X_S^\top\|_{op}^2 = \|X_S\|_{op}^2 \leq \frac{s\mu^2 p}{n} =: \delta < 1$ by (16). Using the Neumann series bound (for all square matrices A such that $\|A\|_{op} < 1$, $\|(I - A)^{-1}\|_{op} \leq 1/(1 - \|A\|_{op})$) and (16), we have that

$$\|(I - X_S^\top X_S)^{-1}\|_{op} \leq \frac{1}{1 - \|X_S^\top X_S\|_{op}} = \frac{1}{1 - \|X_S\|_{op}^2}.$$

It follows that

$$\frac{\|y - X\beta_{-S}\|_2^2}{\|y - X\beta^*\|_2^2} \leq 1 + \|(I - X_S^\top X_S)^{-1}\|_{op}^2 \|X_S^\top\|_{op}^2 \leq 1 + \frac{\delta}{(1 - \delta)^2}.$$

We further have that

$$\delta \leq \frac{\epsilon}{2\epsilon + 1} \leq \frac{2\epsilon + 1 - \sqrt{4\epsilon + 1}}{2\epsilon},$$

where the first inequality follows from (15) and the second from $\epsilon > 0$. This implies $\epsilon\delta^2 - (2\epsilon + 1)\delta + \epsilon \geq 0$ (by analyzing the roots of the left-hand side) and thus $\frac{\delta}{(1 - \delta)^2} \leq \epsilon$. This finishes the proof of Proposition 18. \blacksquare

D.2 Proof of Theorem 5

i) Effect of normalization. We prove the statement by counterexample. Consider two domains $\mathcal{E} := \{1, 2\}$ with population covariance matrices

$$\Sigma_1 := \text{diag}(0.1, 0, 9), \quad \Sigma_2 := \text{diag}(9, 1).$$

$V^{\text{norm-minPCA}}$ solves rank-1 **norm-minPCA** if

$$V^{\text{norm-minPCA}} \in \arg \max_{\substack{v=(a,b) \in \mathbb{R}^2; \\ \|v\|=1}} \left\{ \min(0.1a^2 + 0.9b^2, 0.9a^2 + 0.1b^2) \right\}.$$

The solution equalizes the two terms, hence $V^{\text{norm-minPCA}} = \frac{1}{\sqrt{2}}(1, 1)^\top$ solves **norm-minPCA**.

V^{minPCA} solves rank-1 **minPCA** if

$$V^{\text{minPCA}} \in \arg \max_{\substack{v=(a,b) \in \mathbb{R}^2; \\ \|v\|=1}} \left\{ \min(0.1a^2 + 0.9b^2, 9a^2 + 1b^2) \right\} = \arg \max_{\substack{v=(a,b) \in \mathbb{R}^2; \\ \|v\|=1}} (0.1a^2 + 0.9b^2).$$

Hence $V^{\text{minPCA}} = (0, 1)^\top$ solves **minPCA**. Then,

$$\begin{aligned} \min_{e \in \{1, 2\}} \mathcal{L}_{\text{normVar}}(V^{\text{norm-minPCA}}; \Sigma_e) &= 0.5 > \min_{e \in \{1, 2\}} \mathcal{L}_{\text{normVar}}(V^{\text{minPCA}}; \Sigma_e) = 0.1 \\ \text{and } \min_{e \in \{1, 2\}} \mathcal{L}_{\text{var}}(V^{\text{minPCA}}; \Sigma_e) &= 0.9 > \min_{e \in \{1, 2\}} \mathcal{L}_{\text{var}}(V^{\text{norm-minPCA}}; \Sigma_e) = 0.5. \end{aligned}$$

Hence, V^{minPCA} does not solve **norm-minPCA** and $V^{\text{norm-minPCA}}$ does not solve **minPCA**.

ii) Explained variance vs. reconstruction error. The first claim (that, in general, `minPCA` and `maxRCS` have different solution sets) follows from Example 1. We now show that the solutions of `norm-minPCA` are the same as those of `norm-maxRCS`. Let us begin by simplifying the objective for `norm-maxRCS`:

$$\begin{aligned} \arg \min_{V \in \mathcal{O}_{p \times k}} \left\{ \max_{e \in \mathcal{E}} \frac{\mathbb{E} [\|\mathbf{x}_e - \mathbf{x}_e V V^\top\|_2^2]}{\mathbb{E} [\|\mathbf{x}_e\|_2^2]} \right\} &= \arg \min_{V \in \mathcal{O}_{p \times k}} \left\{ \max_{e \in \mathcal{E}} \frac{\text{Tr}(\Sigma_e) - \text{Tr}(V^\top \Sigma_e V)}{\text{Tr}(\Sigma_e)} \right\} \\ &= \arg \min_{V \in \mathcal{O}_{p \times k}} \left\{ 1 - \min_{e \in \mathcal{E}} \left(\frac{\text{Tr}(V^\top \Sigma_e V)}{\text{Tr}(\Sigma_e)} \right) \right\} \\ &= \arg \max_{V \in \mathcal{O}_{p \times k}} \left\{ \min_{e \in \mathcal{E}} \frac{\text{Tr}(V^\top \Sigma_e V)}{\text{Tr}(\Sigma_e)} \right\}. \end{aligned}$$

The final line is the objective for `norm-minPCA`. Hence, the set of solutions to `norm-minPCA` and `norm-maxRCS` are identical.

iii) Regret. Finally, we verify that the solutions to `maxRegret` are the same whether it is defined via reconstruction error or explained variance. For $V \in \mathcal{O}_{p \times k}$, for all domains $e \in \mathcal{E}$, recall that the explained variance and reconstruction error are, respectively,

$$\begin{aligned} \mathcal{L}_{\text{var}}(V; P_e) &= \text{Tr}(V^\top \Sigma_e V), \\ \mathcal{L}_{\text{RCS}}(V; P_e) &= \mathbb{E} [\|\mathbf{x}_e - \mathbf{x}_e V V^\top\|_2^2] = \text{Tr}(\Sigma_e) - \text{Tr}(V^\top \Sigma_e V) = \text{Tr}(\Sigma_e) - \mathcal{L}_{\text{var}}(V; P_e). \end{aligned}$$

Thus, for any $e \in \mathcal{E}$, the regret is

$$\begin{aligned} \mathcal{L}_{\text{reg}}(V; P_e) &= \mathcal{L}_{\text{RCS}}(V; P_e) - \min_{W \in \mathcal{O}_{p \times k}} \mathcal{L}_{\text{RCS}}(W; P_e) \\ &= (\text{Tr}(\Sigma_e) - \mathcal{L}_{\text{var}}(V; P_e)) - (\text{Tr}(\Sigma_e) - \max_{W \in \mathcal{O}_{p \times k}} \mathcal{L}_{\text{var}}(W; P_e)) \\ &= \max_{W \in \mathcal{O}_{p \times k}} \mathcal{L}_{\text{var}}(W; P_e) - \mathcal{L}_{\text{var}}(V; P_e). \end{aligned}$$

Hence, the regret computed by minimizing reconstruction error is identical to that obtained by maximizing explained variance, and the two formulations therefore yield the same set of optimal solutions. The proof for the normalized case follows from $\mathcal{L}_{\text{normRCS}}(V; P_e) = 1 - \mathcal{L}_{\text{normVar}}(V; P_e)$. \blacksquare

D.3 Proof of Theorem 6

We write the proof for `maxRCS`. The guarantees for the variants `norm-maxRCS`, `minPCA`, and `norm-minPCA` hold with minor modifications to the proof and thus are omitted. The modification for `maxRegret` for Statement i) is given at the end of the proof, from which the subsequent statements and guarantees for `norm-maxRegret` follow.

Let V_k^* solve `maxRCS`. Let $P \in \mathcal{P}$ be any distribution with zero mean and covariance $\Sigma \in \mathcal{C} = \text{conv}(\{\Sigma_e\}_{e \in \mathcal{E}})$. Then, there exist weights $(\mu_e)_{e \in \mathcal{E}}$ such that for all $e \in \mathcal{E}$, $\mu_e \geq 0$, $\sum_{e \in \mathcal{E}} \mu_e = 1$, and

$$\Sigma = \sum_{e \in \mathcal{E}} \mu_e \Sigma_e. \quad (18)$$

Proof of i). For all $P \in \mathcal{P}$ and all $V \in \mathcal{O}_{p \times k}$, the expected reconstruction error is

$$\begin{aligned} \mathcal{L}_{\text{RCS}}(V; P) &= \text{Tr}(\Sigma) - \text{Tr}(V^\top \Sigma V) \\ &= \sum_{e \in \mathcal{E}} \mu_e \left(\text{Tr}(\Sigma_e) - \text{Tr}(V^\top \Sigma_e V) \right) \quad (\text{by (18)}) \\ &= \sum_{e \in \mathcal{E}} \mu_e \mathcal{L}_{\text{RCS}}(V; P_e) \\ &\leq \max_{e \in \mathcal{E}} \mathcal{L}_{\text{RCS}}(V; P_e). \end{aligned}$$

Hence $\sup_{P \in \mathcal{P}} \mathcal{L}_{\text{RCS}}(V; P) \leq \max_{e \in \mathcal{E}} \mathcal{L}_{\text{RCS}}(V; P_e)$. Further, because $\{P_e\}_{e \in \mathcal{E}} \subseteq \mathcal{P}$, it trivially holds that $\max_{e \in \mathcal{E}} \mathcal{L}_{\text{RCS}}(V; P_e) \leq \sup_{P \in \mathcal{P}} \mathcal{L}_{\text{RCS}}(V; P)$. Thus, equality holds.

Proof of ii). Statement i) implies that for all $V_k, W_k \in \mathcal{O}_{p \times k}$, if $\max_{e \in \mathcal{E}} \mathcal{L}_{\text{RCS}}(V_k; P_e) < \max_{e \in \mathcal{E}} \mathcal{L}_{\text{RCS}}(W_k; P_e)$, then $\sup_{P \in \mathcal{P}} \mathcal{L}_{\text{RCS}}(V_k; P) < \sup_{P \in \mathcal{P}} \mathcal{L}_{\text{RCS}}(W_k; P)$.

Proof of iii). Since $\{P_e\}_{e \in \mathcal{E}} \subseteq \mathcal{P}$, we have for all $V \in \mathcal{O}_{p \times k}$,

$$\sup_{P \in \mathcal{P}} \mathcal{L}_{\text{RCS}}(V; P) \geq \max_{e \in \mathcal{E}} \mathcal{L}_{\text{RCS}}(V; P_e) \geq \max_{e \in \mathcal{E}} \mathcal{L}_{\text{RCS}}(V_k^*; P_e) = \sup_{P \in \mathcal{P}} \mathcal{L}_{\text{RCS}}(V_k^*; P),$$

where the second inequality follows by the optimality of V_k^* , and the equality follows from Statement i).

Proof of iv). A counterexample showing that pooled and separate PCA solutions can fail to satisfy Statement iii) is provided in Example 1.

Modification for maxRegret. We show Statement i) for the regret. For all $P \in \mathcal{P}$ and all $V \in \mathcal{O}_{p \times k}$, the expected regret is

$$\begin{aligned} \mathcal{L}_{\text{reg}}(V; P) &= \text{Tr}(\Sigma) - \text{Tr}(V^\top \Sigma V) - \min_{W \in \mathcal{O}_{p \times k}} \{ \text{Tr}(\Sigma) - \text{Tr}(W^\top \Sigma W) \} \\ &= \sum_{e \in \mathcal{E}} \mu_e \left(\text{Tr}(\Sigma_e) - \text{Tr}(V^\top \Sigma_e V) \right) - \min_{W \in \mathcal{O}_{p \times k}} \left\{ \sum_{e \in \mathcal{E}} \mu_e \left(\text{Tr}(\Sigma_e) - \text{Tr}(W^\top \Sigma_e W) \right) \right\} \\ &\leq \sum_{e \in \mathcal{E}} \mu_e \left(\text{Tr}(\Sigma_e) - \text{Tr}(V^\top \Sigma_e V) \right) - \sum_{e \in \mathcal{E}} \mu_e \min_{W \in \mathcal{O}_{p \times k}} \left\{ \left(\text{Tr}(\Sigma_e) - \text{Tr}(W^\top \Sigma_e W) \right) \right\} \\ &= \sum_{e \in \mathcal{E}} \mu_e \mathcal{L}_{\text{reg}}(V; P_e) \leq \max_{e \in \mathcal{E}} \mathcal{L}_{\text{reg}}(V; P_e). \end{aligned}$$

■

D.4 Proof of Proposition 9

Let V_k^* and \hat{V}_k denote the population and empirical solutions, respectively, to any of the considered problems (**minPCA**, **norm-minPCA**, **maxRCS**, **norm-maxRCS**, **maxRegret**, or **norm-maxRegret**), and let \mathcal{L} denote the corresponding loss.⁹ For all $V \in \mathcal{O}_{p \times k}$ and $e \in \mathcal{E}$, let the population and empirical domain-specific objectives be

$$M_e^{\mathcal{L}}(V) := -\mathcal{L}(V; \Sigma_e), \quad \hat{M}_e^{\mathcal{L}}(V) := -\mathcal{L}(V; \hat{\Sigma}_e).$$

9. So $\mathcal{L} \in \{-\mathcal{L}_{\text{var}}, -\mathcal{L}_{\text{normVar}}, \mathcal{L}_{\text{RCS}}, \mathcal{L}_{\text{normRCS}}, \mathcal{L}_{\text{reg}}, \mathcal{L}_{\text{normReg}}\}$, as in Theorems 6 and 7.

Similarly, let the population and empirical worst-case objectives be

$$M^{\mathcal{L}}(V) := \min_{e \in \mathcal{E}} -\mathcal{L}(V; \Sigma_e), \quad \hat{M}^{\mathcal{L}}(V) := \min_{e \in \mathcal{E}} -\mathcal{L}(V; \hat{\Sigma}_e).$$

All six population and empirical estimators can thus be written as $V_k^* \in \arg \max_{V \in \mathcal{O}_{p \times k}} M^{\mathcal{L}}(V)$ and $\hat{V}_k \in \arg \max_{V \in \mathcal{O}_{p \times k}} \hat{M}^{\mathcal{L}}(V)$. As $\mathcal{O}_{p \times k}$ is compact and M and \hat{M} are continuous with respect to the metric induced by the Frobenius norm, the maxima are attained. We now show that

- i) for all $e \in \mathcal{E}$, $\sup_{V \in \mathcal{O}_{p \times k}} |\hat{M}_e^{\mathcal{L}}(V) - M_e^{\mathcal{L}}(V)| \xrightarrow{p} 0$ as $n_e \rightarrow \infty$,
- ii) $\hat{M}^{\mathcal{L}}$ uniformly converges to $M^{\mathcal{L}}$,
- iii) the maximum of $M^{\mathcal{L}}$ is well-separated.

Then, by Theorem 5.7. in van der Vaart (1998), the estimators are consistent, that is, $d(\hat{V}_k, V_k^*) \xrightarrow{p} 0$ as $n_{\min} \rightarrow \infty$.

Proof of i): Domain-specific uniform convergence. We first establish some general bounds. By the law of large numbers, for all $e \in \mathcal{E}$,

$$\|\hat{\Sigma}_e - \Sigma_e\|_F \xrightarrow{p} 0 \quad \text{as } n_e \rightarrow \infty. \quad (19)$$

For all $V \in \mathcal{O}_{p \times k}$, by definition, $\|VV^\top\|_F = \sqrt{\text{Tr}(V^\top V)} = \sqrt{\text{Tr}(I_k)} = \sqrt{k}$ and $\|I_p\|_F = \sqrt{p}$. Hence, by Cauchy-Schwarz, for all $V \in \mathcal{O}_{p \times k}$,

$$|\text{Tr}(V^\top [\hat{\Sigma}_e - \Sigma_e] V)| \leq \sqrt{k} \|\hat{\Sigma}_e - \Sigma_e\|_F, \quad (20)$$

$$|\text{Tr}(\hat{\Sigma}_e - \Sigma_e)| \leq \|I_p\|_F \|\hat{\Sigma}_e - \Sigma_e\|_F = \sqrt{p} \|\hat{\Sigma}_e - \Sigma_e\|_F. \quad (21)$$

We now apply these bounds to each specific objective function.

Case 1: minPCA. By (20), we have that for all $e \in \mathcal{E}$ and for all $V \in \mathcal{O}_{p \times k}$,

$$|\hat{M}_e^{\mathcal{L}}(V) - M_e^{\mathcal{L}}(V)| = |\text{Tr}(V^\top [\hat{\Sigma}_e - \Sigma_e] V)| \leq \sqrt{k} \|\hat{\Sigma}_e - \Sigma_e\|_F.$$

Hence, for all $e \in \mathcal{E}$, $\sup_{V \in \mathcal{O}_{p \times k}} |\hat{M}_e^{\mathcal{L}}(V) - M_e^{\mathcal{L}}(V)| \leq \sqrt{k} \|\hat{\Sigma}_e - \Sigma_e\|_F \xrightarrow{p} 0$ as $n_e \rightarrow \infty$ by (19).

Case 2: maxRCS. By (20) and (21), we have that for all $e \in \mathcal{E}$ and for all $V \in \mathcal{O}_{p \times k}$,

$$|\hat{M}_e^{\mathcal{L}}(V) - M_e^{\mathcal{L}}(V)| \leq |\text{Tr}(V^\top [\hat{\Sigma}_e - \Sigma_e] V)| + |\text{Tr}(\hat{\Sigma}_e - \Sigma_e)| \leq (\sqrt{k} + \sqrt{p}) \|\hat{\Sigma}_e - \Sigma_e\|_F.$$

Hence, for all $e \in \mathcal{E}$, $\sup_{V \in \mathcal{O}_{p \times k}} |\hat{M}_e^{\mathcal{L}}(V) - M_e^{\mathcal{L}}(V)| \leq (\sqrt{k} + \sqrt{p}) \|\hat{\Sigma}_e - \Sigma_e\|_F \xrightarrow{p} 0$ as $n_e \rightarrow \infty$.

Case 3: norm-minPCA. Let $\tau := \min_{e \in \mathcal{E}} \text{Tr}(\Sigma_e) > 0$. Then, gathering (20), (21), and using that $\text{Tr}(V^\top \hat{\Sigma}_e V) \leq \text{Tr}(\hat{\Sigma}_e)$ (indeed, as $I - VV^\top$ and $\hat{\Sigma}_e$ are positive semi-definite, we

have $\text{Tr}(\hat{\Sigma}_e - \hat{\Sigma}_e V V^\top) \geq 0$, we have that for all $e \in \mathcal{E}$ and for all $V \in \mathcal{O}_{p \times k}$,

$$\begin{aligned}
 |\hat{M}_e^{\mathcal{L}}(V) - M_e^{\mathcal{L}}(V)| &= \left| \frac{\text{Tr}(V^\top \hat{\Sigma}_e V)}{\text{Tr}(\hat{\Sigma}_e)} - \frac{\text{Tr}(V^\top \Sigma_e V)}{\text{Tr}(\Sigma_e)} \right| \\
 &\leq \frac{|\text{Tr}(V^\top [\hat{\Sigma}_e - \Sigma_e] V)|}{\text{Tr}(\Sigma_e)} + \text{Tr}(V^\top \hat{\Sigma}_e V) \left| \frac{1}{\text{Tr}(\hat{\Sigma}_e)} - \frac{1}{\text{Tr}(\Sigma_e)} \right| \\
 &\leq \frac{|\text{Tr}(V^\top [\hat{\Sigma}_e - \Sigma_e] V)|}{\text{Tr}(\Sigma_e)} + \text{Tr}(V^\top \hat{\Sigma}_e V) \frac{|\text{Tr}(\hat{\Sigma}_e - \Sigma_e)|}{\text{Tr}(\hat{\Sigma}_e) \text{Tr}(\Sigma_e)} \\
 &\leq \frac{|\text{Tr}(V^\top [\hat{\Sigma}_e - \Sigma_e] V)|}{\text{Tr}(\Sigma_e)} + \text{Tr}(\hat{\Sigma}_e) \frac{|\text{Tr}(\hat{\Sigma}_e - \Sigma_e)|}{\text{Tr}(\hat{\Sigma}_e) \text{Tr}(\Sigma_e)} \\
 &\leq \frac{\sqrt{k} + \sqrt{p}}{\tau} \|\hat{\Sigma}_e - \Sigma_e\|_F. \tag{22}
 \end{aligned}$$

Thus, $\sup_{V \in \mathcal{O}_{p \times k}} |\hat{M}_e^{\mathcal{L}}(V) - M_e^{\mathcal{L}}(V)| \leq \frac{\sqrt{k} + \sqrt{p}}{\tau} \|\hat{\Sigma}_e - \Sigma_e\|_F \xrightarrow{p} 0$ as $n_e \rightarrow \infty$.

Case 4: norm-maxRCS. By Theorem 5i), the solutions of population **norm-minPCA** and population **norm-maxRCS** coincide; the same algebra shows the solutions of the empirical problems also coincide. Thus, the consistency of **norm-minPCA** implies the consistency of **norm-maxRCS**.

Case 5: maxRegret. For all $e \in \mathcal{E}$ and for all $V \in \mathcal{O}_{p \times k}$, consider

$$\begin{aligned}
 |\hat{M}_e^{\mathcal{L}}(V) - M_e^{\mathcal{L}}(V)| &= \left| \text{Tr}(V^\top \hat{\Sigma}_e V) - \max_{W \in \mathcal{O}_{p \times k}} \text{Tr}(W^\top \hat{\Sigma}_e W) - \left\{ \text{Tr}(V^\top \Sigma_e V) - \max_{W \in \mathcal{O}_{p \times k}} \text{Tr}(W^\top \Sigma_e W) \right\} \right| \\
 &\leq \underbrace{\left| \text{Tr}(V^\top \hat{\Sigma}_e V) - \text{Tr}(V^\top \Sigma_e V) \right|}_{=:A} + \underbrace{\left| \sum_{i=1}^k \lambda_i(\hat{\Sigma}_e) - \sum_{i=1}^k \lambda_i(\Sigma_e) \right|}_{=:B},
 \end{aligned}$$

where $\lambda_i(\cdot)$ gives the i -th largest eigenvalue. By (20), $A \leq \sqrt{k} \|\hat{\Sigma}_e - \Sigma_e\|_F$ and by Weyl's inequality for symmetric matrices (e.g., Theorem 4.3.1 in Horn and Johnson, 1985)

$$B \leq k \|\hat{\Sigma}_e - \Sigma_e\|_{\text{op}} \leq k \|\hat{\Sigma}_e - \Sigma_e\|_F. \tag{23}$$

Hence, $\sup_{V \in \mathcal{O}_{p \times k}} |\hat{M}_e^{\mathcal{L}}(V) - M_e^{\mathcal{L}}(V)| \leq (\sqrt{k} + k) \|\hat{\Sigma}_e - \Sigma_e\|_F \xrightarrow{p} 0$ as $n_{\min} \rightarrow \infty$.

Case 6: norm-maxRegret. By the triangle inequality, for all $e \in \mathcal{E}$ and for all $V \in \mathcal{O}_{p \times k}$, $|\hat{M}_e^{\mathcal{L}}(V) - M_e^{\mathcal{L}}(V)|$ is bounded by

$$\left| \frac{\text{Tr}(V^\top \hat{\Sigma}_e V)}{\text{Tr}(\hat{\Sigma}_e)} - \frac{\text{Tr}(V^\top \Sigma_e V)}{\text{Tr}(\Sigma_e)} \right| + \left| \max_{W \in \mathcal{O}_{p \times k}} \frac{\text{Tr}(W^\top \hat{\Sigma}_e W)}{\text{Tr}(\hat{\Sigma}_e)} - \max_{W \in \mathcal{O}_{p \times k}} \frac{\text{Tr}(W^\top \Sigma_e W)}{\text{Tr}(\Sigma_e)} \right|.$$

The first term is bounded by $\frac{\sqrt{k+\sqrt{p}}}{\tau} \|\hat{\Sigma}_e - \Sigma_e\|_F$ exactly as in (22). Following a similar algebraic sequence as in (22), the second term is bounded by

$$\begin{aligned} & \frac{1}{\text{Tr}(\hat{\Sigma}_e)} \left| \max_{W \in \mathcal{O}_{p \times k}} \text{Tr}(W^\top \hat{\Sigma}_e W) - \max_{W \in \mathcal{O}_{p \times k}} \text{Tr}(W^\top \Sigma_e W) \right| + \max_{W \in \mathcal{O}_{p \times k}} \text{Tr}(W^\top \hat{\Sigma}_e W) \left| \frac{1}{\text{Tr}(\hat{\Sigma}_e)} - \frac{1}{\text{Tr}(\Sigma_e)} \right| \\ & \leq \frac{k}{\tau} \|\hat{\Sigma}_e - \Sigma_e\|_{\text{op}} + \text{Tr}(\hat{\Sigma}_e) \left| \frac{\text{Tr}(\hat{\Sigma}_e - \Sigma_e)}{\text{Tr}(\hat{\Sigma}_e) \text{Tr}(\Sigma_e)} \right| \\ & \leq \frac{k+\sqrt{p}}{\tau} \|\hat{\Sigma}_e - \Sigma_e\|_F, \end{aligned} \quad (24)$$

where the first inequality follows from Weyl's inequality (as in case 5) as τ is still defined as $\min_{e \in \mathcal{E}} \text{Tr}(\Sigma_e)$. Hence, $\sup_{V \in \mathcal{O}_{p \times k}} |\hat{M}_e^\mathcal{L}(V) - M_e^\mathcal{L}(V)| \leq \left(\frac{k+\sqrt{k+2\sqrt{p}}}{\tau} \right) \|\hat{\Sigma}_e - \Sigma_e\|_F \xrightarrow{p} 0$ as $n_e \rightarrow \infty$.

Proof of ii). We show that $\hat{M}^\mathcal{L}$ uniformly converges to $M^\mathcal{L}$ by bounding

$$\begin{aligned} \sup_{V \in \mathcal{O}_{p \times k}} |\hat{M}^\mathcal{L}(V) - M^\mathcal{L}(V)| &= \sup_{V \in \mathcal{O}_{p \times k}} \left| \min_{e \in \mathcal{E}} \hat{M}_e^\mathcal{L}(V) - \min_{e \in \mathcal{E}} M_e^\mathcal{L}(V) \right| \\ &\leq \sup_{V \in \mathcal{O}_{p \times k}} \max_{e \in \mathcal{E}} |\hat{M}_e^\mathcal{L}(V) - M_e^\mathcal{L}(V)| \\ &= \max_{e \in \mathcal{E}} \sup_{V \in \mathcal{O}_{p \times k}} |\hat{M}_e^\mathcal{L}(V) - M_e^\mathcal{L}(V)|. \end{aligned}$$

As \mathcal{E} is finite, Statement i) implies that $\sup_{V \in \mathcal{O}_{p \times k}} |\hat{M}^\mathcal{L}(V) - M^\mathcal{L}(V)| \xrightarrow{p} 0$ as $n_{\min} \rightarrow \infty$.

Proof of iii). Consider Assumption 1 and assume by contradiction that the maximum is not well-separated, i.e., there exists $\epsilon > 0$ with $\sup_{V \in \mathcal{O}_{p \times k}; d(V, V_k^*) > \epsilon} M^\mathcal{L}(V) = M^\mathcal{L}(V_k^*)$. This implies that there exists a sequence $(V_n)_{n \in \mathbb{N}}$ in $\mathcal{O}_{p \times k}$ with $\lim_{n \rightarrow \infty} M^\mathcal{L}(V_n) = M^\mathcal{L}(V_k^*)$ and $\forall n \in \mathbb{N}, d(V_n, V_k^*) > \epsilon$. Since $\mathcal{O}_{p \times k}$ is compact under the standard metric induced by the Frobenius norm, the Bolzano–Weierstrass theorem guarantees the existence of a convergent (w.r.t. the standard metric) subsequence of $(V_n)_{n \in \mathbb{N}}$ with limit $\tilde{V} \in \mathcal{O}_{p \times k}$. Because d is continuous with respect to this standard metric, taking the limit yields

$$d(\tilde{V}, V_k^*) \geq \epsilon. \quad (25)$$

Continuity of $M^\mathcal{L}$ then implies $M^\mathcal{L}(\tilde{V}) = M^\mathcal{L}(V_k^*)$. By Assumption 1, there exists $Q \in \mathbb{R}^{k \times k}$ with $Q^\top Q = Q Q^\top = I_k$ such that $\tilde{V} = V_k^* Q$. Hence, $d(\tilde{V}, V_k^*) = 0$ contradicting (25). Thus, the maximum is a well-separated point. \blacksquare

D.5 Proof of Proposition 10

Fix any of the considered problems (minPCA, norm-minPCA, maxRCS, norm-maxRCS, maxRegret, or norm-maxRegret), let \mathcal{L} denote the corresponding loss, and let V_k^* and \hat{V}_k denote population and empirical solutions, respectively.

Proof of i). By Theorems 6 and 7,

$$\sup_{P \in \mathcal{Q}} \mathcal{L}(\hat{V}_k; P) = \max_{e \in \mathcal{E}} \mathcal{L}(\hat{V}_k; \Sigma_e), \quad \sup_{P \in \mathcal{Q}} \mathcal{L}(V_k^*; P) = \max_{e \in \mathcal{E}} \mathcal{L}(V_k^*; \Sigma_e). \quad (26)$$

For all $V, W \in \mathcal{O}_{p \times k}$ and for all $e \in \mathcal{E}$, the map $V \mapsto \mathcal{L}(V; \Sigma_e)$ is c_e -Lipschitz with respect to the projection distance $d(V, W) = \|VV^\top - WW^\top\|_F$, where

$$c_e := \begin{cases} \|\Sigma_e\|_F & \text{for minPCA, maxRCS, maxRegret} \\ \frac{\|\Sigma_e\|_F}{\text{Tr}(\Sigma_e)} & \text{for norm-minPCA, norm-maxRCS, norm-maxRegret.} \end{cases}$$

To see this, consider minPCA. For all $e \in \mathcal{E}$ and for all $V, W \in \mathcal{O}_{p \times k}$

$$\begin{aligned} |\mathcal{L}_{\text{var}}(V; \Sigma_e) - \mathcal{L}_{\text{var}}(W; \Sigma_e)| &= |\text{Tr}(V^\top \Sigma_e V) - \text{Tr}(W^\top \Sigma_e W)| \\ &= |\text{Tr}(\Sigma_e(VV^\top - WW^\top))| \\ &\leq \|\Sigma_e\|_F \|VV^\top - WW^\top\|_F = \|\Sigma_e\|_F d(V, W), \end{aligned}$$

by Cauchy–Schwarz and cyclicity of the trace. For maxRCS and maxRegret, the objectives differ from $\mathcal{L}_{\text{var}}(V; \Sigma_e)$ only by additive terms independent of V , so the same bound applies. The normalized variants introduce only the multiplicative factor $1/\text{Tr}(\Sigma_e)$. This concludes the Lipschitz argument. The maximum of Lipschitz functions is Lipschitz, in this case with constant equal to $\max_{e \in \mathcal{E}} c_e$. Therefore, for all $V, W \in \mathcal{O}_{p \times k}$,

$$\left| \max_{e \in \mathcal{E}} \mathcal{L}(V; \Sigma_e) - \max_{e \in \mathcal{E}} \mathcal{L}(W; \Sigma_e) \right| \leq \left(\max_{e \in \mathcal{E}} c_e \right) d(V, W). \quad (27)$$

Combining (26) with the Lipschitz bound (27) at $V = \hat{V}_k$, $W = V_k^*$ yields

$$\left| \sup_{P \in \mathcal{Q}} \mathcal{L}(\hat{V}_k; P) - \sup_{P \in \mathcal{Q}} \mathcal{L}(V_k^*; P) \right| \leq \left(\max_{e \in \mathcal{E}} c_e \right) d(\hat{V}_k, V_k^*).$$

Since $d(\hat{V}_k, V_k^*) \xrightarrow{p} 0$ as $n_{\min} \rightarrow \infty$ by Proposition 9, the right-hand side converges in probability to zero, proving Statement i).

Proof of ii). It is sufficient to show that

$$\left| \sup_{P \in \mathcal{Q}} \mathcal{L}(\hat{V}_k; P) - \hat{m}_k \right| \xrightarrow{p} 0 \quad \text{as } n_{\min} \rightarrow \infty,$$

where $\hat{m}_k = \max_{e \in \mathcal{E}} \mathcal{L}(\hat{V}_k; \hat{\Sigma}_e)$. By (26), we have that

$$\left| \sup_{P \in \mathcal{Q}} \mathcal{L}(\hat{V}_k; P) - \hat{m}_k \right| = \left| \max_{e \in \mathcal{E}} \mathcal{L}(\hat{V}_k; \Sigma_e) - \max_{e \in \mathcal{E}} \mathcal{L}(\hat{V}_k; \hat{\Sigma}_e) \right| \leq \max_{e \in \mathcal{E}} \left| \mathcal{L}(\hat{V}_k; \Sigma_e) - \mathcal{L}(\hat{V}_k; \hat{\Sigma}_e) \right|.$$

We bound the final term for each of the objectives, using arguments that are analogous to the proof of i) in the proof of Proposition 9. For minPCA, by (20),

$$\begin{aligned} \max_{e \in \mathcal{E}} \left| \mathcal{L}_{\text{var}}(\hat{V}_k; \Sigma_e) - \mathcal{L}_{\text{var}}(\hat{V}_k; \hat{\Sigma}_e) \right| &= \max_{e \in \mathcal{E}} \left| \text{Tr}(\hat{V}_k^\top \Sigma_e \hat{V}_k) - \text{Tr}(\hat{V}_k^\top \hat{\Sigma}_e \hat{V}_k) \right| \\ &\leq \sqrt{k} \max_{e \in \mathcal{E}} \|\Sigma_e - \hat{\Sigma}_e\|_F. \end{aligned} \quad (28)$$

Similarly, for maxRCS, by the cyclic property of the trace,

$$\begin{aligned} \max_{e \in \mathcal{E}} \left| \mathcal{L}_{\text{RCS}}(\hat{V}_k; \Sigma_e) - \mathcal{L}_{\text{RCS}}(\hat{V}_k; \hat{\Sigma}_e) \right| &= \max_{e \in \mathcal{E}} \left| \text{Tr}((\Sigma_e - \hat{\Sigma}_e)(I - \hat{V}_k \hat{V}_k^\top)) \right| \\ &\leq \sqrt{p-k} \max_{e \in \mathcal{E}} \|\Sigma_e - \hat{\Sigma}_e\|_F, \end{aligned}$$

where $\|I - \hat{V}_k \hat{V}_k^\top\|_F = \sqrt{p-k}$ as it is an orthogonal projector of rank $p-k$. Let $\tau := \min_{e \in \mathcal{E}} \text{Tr}(\Sigma_e) > 0$. Then for **norm-minPCA** and **norm-maxRCS**,

$$\begin{aligned} \max_{e \in \mathcal{E}} \left| \mathcal{L}_{\text{normVar}}(\hat{V}_k; \Sigma_e) - \mathcal{L}_{\text{normVar}}(\hat{V}_k; \hat{\Sigma}_e) \right| &= \max_{e \in \mathcal{E}} \left| \mathcal{L}_{\text{normRCS}}(\hat{V}_k; \Sigma_e) - \mathcal{L}_{\text{normRCS}}(\hat{V}_k; \hat{\Sigma}_e) \right| \\ &= \max_{e \in \mathcal{E}} \left| \frac{\text{Tr}(\hat{V}_k^\top \hat{\Sigma}_e \hat{V}_k)}{\text{Tr}(\hat{\Sigma}_e)} - \frac{\text{Tr}(\hat{V}_k^\top \Sigma_e \hat{V}_k)}{\text{Tr}(\Sigma_e)} \right| \\ &\leq \frac{\sqrt{k} + \sqrt{p}}{\tau} \max_{e \in \mathcal{E}} \|\hat{\Sigma}_e - \Sigma_e\|_F, \end{aligned}$$

where the last inequality follows from (22). For **maxRegret**,

$$\begin{aligned} \max_{e \in \mathcal{E}} \left| \mathcal{L}_{\text{reg}}(\hat{V}_k; \Sigma_e) - \mathcal{L}_{\text{reg}}(\hat{V}_k; \hat{\Sigma}_e) \right| &= \max_{e \in \mathcal{E}} \left| \max_{W \in \mathcal{O}_{p \times k}} \text{Tr}(W^\top \Sigma_e W) - \text{Tr}(\hat{V}_k^\top \Sigma_e \hat{V}_k) - \max_{W \in \mathcal{O}_{p \times k}} \text{Tr}(W^\top \hat{\Sigma}_e W) + \text{Tr}(\hat{V}_k^\top \hat{\Sigma}_e \hat{V}_k) \right| \\ &\leq \max_{e \in \mathcal{E}} \left| \max_{W \in \mathcal{O}_{p \times k}} \text{Tr}(W^\top \Sigma_e W) - \max_{W \in \mathcal{O}_{p \times k}} \text{Tr}(W^\top \hat{\Sigma}_e W) \right| + \max_{e \in \mathcal{E}} \left| \text{Tr}(\hat{V}_k^\top \Sigma_e \hat{V}_k) - \text{Tr}(\hat{V}_k^\top \hat{\Sigma}_e \hat{V}_k) \right| \\ &= \max_{e \in \mathcal{E}} \left| \sum_{i=1}^k \lambda_i(\Sigma_e) - \sum_{i=1}^k \lambda_i(\hat{\Sigma}_e) \right| + \max_{e \in \mathcal{E}} \left| \text{Tr}(\hat{V}_k^\top \Sigma_e \hat{V}_k) - \text{Tr}(\hat{V}_k^\top \hat{\Sigma}_e \hat{V}_k) \right| \\ &\leq (k + \sqrt{k}) \max_{e \in \mathcal{E}} \|\Sigma_e - \hat{\Sigma}_e\|_F, \end{aligned}$$

where the last inequality follows as in (23). Finally, for **norm-maxRegret**, as in case 6 of the proof of Proposition 9,

$$\max_{e \in \mathcal{E}} \left| \mathcal{L}_{\text{normReg}}(\hat{V}_k; \Sigma_e) - \mathcal{L}_{\text{normReg}}(\hat{V}_k; \hat{\Sigma}_e) \right| \leq \frac{k + \sqrt{k} + 2\sqrt{p}}{\tau} \max_{e \in \mathcal{E}} \|\hat{\Sigma}_e - \Sigma_e\|_F.$$

Since \mathcal{E} is finite and for all $e \in \mathcal{E}$ we have $\|\hat{\Sigma}_e - \Sigma_e\|_F \xrightarrow{p} 0$ as $n_e \rightarrow \infty$ (by (19)), it follows that

$$\max_{e \in \mathcal{E}} \|\hat{\Sigma}_e - \Sigma_e\|_F \xrightarrow{p} 0 \quad \text{as } n_{\min} \rightarrow \infty,$$

which proves Statement ii). ■

D.6 Proof of Theorem 13

Let $V_k^* \in \mathcal{O}_{p \times k}$ be a rank- k solution to **maxRCS** and assume V_k^* is μ -incoherent. Fix $\mathbf{x} \in \mathbb{R}^{1 \times p}$ and a mask $\omega \in \{0, 1\}^p$ such that the number s of unobserved entries satisfies $s \leq \frac{p\epsilon}{k\mu^2(2\epsilon+1)}$ and let $S(\omega) := \{i \in [p] : \omega_i = 0\}$ denote the set of unobserved coordinates. Inductive matrix completion via least squares is equivalent to ordinary least squares of the response $y := \mathbf{x}^\top$ on the design matrix $X := V_k^*$, with the rows indexed by $S(\omega)$ removed. Hence, Proposition 18 (Appendix D.1) applies with

$$X := V_k^* \in \mathbb{R}^{p \times k}, \quad y := \mathbf{x}^\top \in \mathbb{R}^p, \quad S := S(\omega),$$

which yields¹⁰

$$\|\mathbf{x} - \ell(\mathbf{x}, \omega, V_k^*)(V_k^*)^\top\|_2^2 \leq (1 + \epsilon) \|\mathbf{x} - \mathbf{x} V_k^* (V_k^*)^\top\|_2^2.$$

10. This is the transpose-version of Proposition 18; the Euclidean norm is invariant under transposition.

Since $s \leq \frac{p\epsilon}{k\mu^2(2\epsilon+1)}$ holds Q -almost surely by Assumption 2, the above inequality holds Q -almost surely for $\omega \sim Q$. For any $P \in \mathcal{P}$, we then take expectations over $\mathbf{x} \sim P$ and $\omega \sim Q$, yielding

$$\begin{aligned} \mathcal{L}_{P,Q}(V_k^*) &= \mathbb{E}_{\mathbf{x} \sim P, \omega \sim Q} \|\mathbf{x} - \ell(\mathbf{x}, \omega, V_k^*)(V_k^*)^\top\|_2^2 \\ &\leq (1 + \epsilon) \mathbb{E}_{\mathbf{x} \sim P, \omega \sim Q} \|\mathbf{x} - \mathbf{x}V_k^*(V_k^*)^\top\|_2^2 = (1 + \epsilon) \mathbb{E}_{\mathbf{x} \sim P} \|\mathbf{x} - \mathbf{x}V_k^*(V_k^*)^\top\|_2^2. \end{aligned}$$

Taking the supremum over $P \in \mathcal{P}$ and applying statement (i) of Theorem 6 gives

$$\begin{aligned} \sup_{P \in \mathcal{P}} \mathcal{L}_{P,Q}(V_k^*) &\leq (1 + \epsilon) \sup_{P \in \mathcal{P}} \mathbb{E}_{\mathbf{x} \sim P} \|\mathbf{x} - \mathbf{x}V_k^*(V_k^*)^\top\|_2^2 \\ &= (1 + \epsilon) \max_{e \in \mathcal{E}} \mathbb{E}_{\mathbf{x} \sim P_e} \|\mathbf{x} - \mathbf{x}V_k^*(V_k^*)^\top\|_2^2 \\ &= (1 + \epsilon) \min_{V \in \mathcal{O}_{p \times k}} \max_{e \in \mathcal{E}} \mathbb{E}_{\mathbf{x} \sim P_e} \|\mathbf{x} - \mathbf{x}VV^\top\|_2^2, \end{aligned} \tag{29}$$

where the last equality follows from the definition of V_k^* as a rank- k solution to \mathbf{maxRCS} . Finally, for any fixed \mathbf{x} and $V \in \mathcal{O}_{p \times k}$, the choice $\ell = \mathbf{x}V$ minimizes $\|\mathbf{x} - \ell V^\top\|_2^2$ over $\ell \in \mathbb{R}^k$. Hence, for all \mathbf{x} and for all ω ,

$$\|\mathbf{x} - \mathbf{x}VV^\top\|_2^2 \leq \|\mathbf{x} - \ell(\mathbf{x}, \omega, V)V^\top\|_2^2,$$

and therefore for each domain e ,

$$\mathbb{E}_{\mathbf{x} \sim P_e} \|\mathbf{x} - \mathbf{x}VV^\top\|_2^2 \leq \mathbb{E}_{\mathbf{x} \sim P_e, \omega \sim Q} \|\mathbf{x} - \ell(\mathbf{x}, \omega, V)V^\top\|_2^2 \leq \sup_{P \in \mathcal{P}} \mathcal{L}_{P,Q}(V).$$

Taking the maximum over $e \in \mathcal{E}$ and then the minimum over $V \in \mathcal{O}_{p \times k}$ gives

$$\min_{V \in \mathcal{O}_{p \times k}} \max_{e \in \mathcal{E}} \mathbb{E}_{\mathbf{x} \sim P_e} \|\mathbf{x} - \mathbf{x}VV^\top\|_2^2 \leq \min_{V \in \mathcal{O}_{p \times k}} \sup_{P \in \mathcal{P}} \mathcal{L}_{P,Q}(V).$$

Combining this identity with (29) yields

$$\sup_{P \in \mathcal{P}} \mathcal{L}_{P,Q}(V_k^*) \leq (1 + \epsilon) \min_{V \in \mathcal{O}_{p \times k}} \sup_{P \in \mathcal{P}} \mathcal{L}_{P,Q}(V).$$

as claimed. ■